Naval Research Laboratory
Stennis Space Center, MS 39529-5004

NRL/FR/7322--97-9675

Joint Distributed Surf Zone Environmental Model: FY96 Modeling Procedure

Richard A. Allard

Ocean Dynamics and Prediction Branch
Oceanography Division

Mona J. Collins
Donald R. Del Balzo

Acoustic Simulation and Tactics Branch
Acoustics Division

Jane McKee Smith

Research Division
Coastal and Hydraulics Laboratory
Vicksburg, MS

December 22, 1997

REPORT DOCUMENTATION PAGE

Form Approved
OBM No. 0704-0188

1. AGENCY USE ONLY *(Leave blank)*

2. REPORT DATE
December 22, 1997

3. REPORT TYPE AND DATES COVERED
Final

4. TITLE AND SUBTITLE
Joint Distributed Surf Zone Environmental Model: FY96 Modeling Procedure

5. FUNDING NUMBERS
Job Order No. 573-7254-00
Program Element No. 06038320
Project No.
Task No. DMSO-97-0082
Accession No.

6. AUTHOR(S)
Richard A. Allard, Mona J. Collins, Donald R. Del Balzo, and Jane McKee Smith*

7. PERFORMING ORGANIZATION NAME(S) AND ADDRESS(ES)
Naval Research Laboratory
Oceanography Division
Stennis Space Center, MS 39529-5004

8. PERFORMING ORGANIZATION REPORT NUMBER
NRL/FR/7322--97-9675

9. SPONSORING/MONITORING AGENCY NAME(S) AND ADDRESS(ES)
DoD Washington Headquarters Services
Installation Accounting Division
1155 Defense Pentagon, Room BB269
Washington, DC 20301-1155

10. SPONSORING/MONITORING AGENCY REPORT NUMBER

11. SUPPLEMENTARY NOTES
*Coastal and Hydraulics Laboratory, Research Division, Vicksburg, MS

12a. DISTRIBUTION/AVAILABILITY STATEMENT
Approved for public release; distribution unlimited.

12b. DISTRIBUTION CODE

13. ABSTRACT *(Maximum 200 words)*

This report documents the modeling procedure used during the FY96 Joint Distributed Surf Zone Environmental Model Program. The approach of this program is to develop techniques that incorporate current state-of-art, physics-based numerical models to determine surf zone characteristic that are important to the modeling and simulation community. To test this proof of concept, a suite of models were identified and tested for Camp Pendelton, CA, during two 7-day periods in January and August 1995, in which data from the Coupled Ocean Atmosphere Mesoscale Prediction System (COAMPS) and the deep-water wave model WAM, were available. Spectra describing the wave energy distribution in both frequency and direction were obtained from the Southern California Regional WAM model and specified on the offshore boundary of the STWAVE shallow-water wave model. STWAVE was run to coincide with the time period of available WAM and COAMPS data. The Navy Standard Surf Model (NSSM) was run for the Camp Pendleton area for the same periods that WAM and STWAVE were run: 8–14 Jan and 18–24 Aug 1995. A refraction zone depth grid was built from a 100-m resolution bathymetric data base. Inputs included COAMPS wind speed and direction, tide levels from tide tables, WAM spectra, and a landing zone based on a linear beach slope of 0.007. WAM, STWAVE, and NSSM model outputs described in this report are available to the Modeling and Simulation community through the Master Environmental Library (http://mel.dmso.mil).

14. SUBJECT TERMS
surf zone, oceanographic data, environmental data access

15. NUMBER OF PAGES
46

16. PRICE CODE

17. SECURITY CLASSIFICATION OF REPORT	18. SECURITY CLASSIFICATION OF THIS PAGE	19. SECURITY CLASSIFICATION OF ABSTRACT	20. LIMITATION OF ABSTRACT
Unclassified	Unclassified	Unclassified	Same as report

NSN 7540-01-280-5500

Standard Form 298 (Rev. 2-89)
Prescribed by ANSI Std. Z39-18
298-102

INTRODUCTION AND OVERVIEW

This Report covers recent NRL research and development related to the AEC laser-pellet fusion program. The work covered in this report was primarily carried out under AEC Contract No. AT(04-3)-878 between July, 1973 and June, 1974. In some cases, for the sake of clarity, work not performed during this period has been included. In addition, the report discusses the large complementary program supported by the Defense Nuclear Agency at NRL on the study of laser produced plasmas in high atomic number materials. A significant part of the soft x-ray experimental studies (Chapter V) and all of the numerical modelling studies (Chapter VIII and Chapter IX) were supported by the DNA program. This work has been included in the present report for the sake of completeness and since many of the results obtained are of direct benefit to the AEC laser-fusion effort.

There is some overlap in time, with the period covered by the last NRL report, which was presented to the Laser-Fusion Coordinating Committee in November, 1973. However, it was felt useful to establish the precedent of fiscal year reporting starting with this Annual Report. In the future, a report on the AEC supported laser-fusion studies at NRL will appear on a semi-annual basis.

Studies of laser produced plasmas began at NRL in 1968. Development of a large Q-switched glass laser facility was carried out under ARPA sponsorship. Additional support for laser development was received as part of a DNA-supported program to study the interactions between an expanding laser-produced plasma and an ambient magnetized plasma background. The DNA program also provided NRL with the genesis of its expertise in the study of laser plasma generation and interactions. The glass laser system was developed under joint ARPA and DNA sponsorship to the point where, by FY 72, it represented the state-of-the-art in high power short pulse lasers. The system included an NRL designed mode-locked YAG oscillator system and a disc amplifier which became a prototype for those now in use and under development in the laser-fusion program.

When a large AEC supported laser-fusion effort began in FY 72, NRL was a logical place to turn to for support in building up the programs of the AEC laboratories. Shortly after the start of AEC-supported work at NRL, a DNA program at NRL was initiated to study laser produced high atomic number plasmas. The aim of this program was to develop a new source of soft x-rays for weapons effect simulation. The combined AEC and DNA supported programs have been known within NRL as the Laser-Matter Interaction (LMI) Program and Dr. John Stamper has served as Program Manager since its inception. The LMI Program has included contributions from a number of divisions at NRL and has involved both experimental and theoretical studies. The funding of the program during FY 74 consisted of \$500,000 from the AEC for laser-fusion studies as well as additional funding from DNA for x-ray source investigations.

One of the unique features of the NRL laser-fusion program has been the availability of a reliable Nd:glass laser system which produces exceptionally clean pulses (i.e., spatially, temporally and spectrally pure) at sufficient power levels ($\lesssim$ 0.5 TW) for many studies of interest to laser fusion. Over 1500 laser shots were put on target in FY 74 for our AEC

CONTENTS

JOINT DISTRIBUTED SURF ZONE ENVIRONMENTAL MODEL: FY96 MODELING PROCEDURE

1.0 INTRODUCTION

In response to new modeling and simulation requirements for littoral warfare, a project was initiated in FY96 to construct an environmental description of physical processes in the surf zone. The sponsors are the Ocean Executive Agent (OEA) and the Defense Modeling Simulation Office (DMSO). This new project is called the Joint Distributed Surf Zone Environmental Model (JDSZEM). The primary performers in FY96 were the Naval Surface Warfare Center (NSWC) in Panama City, FL, the Naval Research Laboratory (NRL) at Stennis Space Center, MS, and the Army Coastal and Hydraulics Laboratory (CHL) in Vicksburg, MS. NSWC focused on feature modeling and environmental requirements for systems operating in the surf zone. NRL and CHL combined efforts to produce an environmental description of surf zone processes.

This report documents the environmental modeling procedures used in the JDSZEM effort. A series of numerical models were employed to determine the surf zone characteristics near Camp Pendleton, CA, during two 1-wk periods in January and August 1995. The results of this effort were to be ingested into the Master Environmental Library (MEL) and made available to the Total Atmosphere Ocean Server (TAOS) for the Synthetic Environment (SE) 4 Demonstration that took place in September 1996. The JDSZEM intent is not to support specific programs; rather, the approach is to develop techniques that incorporate the current *off-the-shelf* physics-based numerical models to determine nearshore and surf zone characteristics that are important to the modeling and simulation community. For example, the two-dimensional (2-D) wave spectrum from a shallow-water wave model could be used to construct realistic water surface representations for environmental simulations. This information could also be used to model vehicle dynamic behavior in shallow water. When possible, JDSZEM tries to interact with other programs to demonstrate the applicability of the techniques being developed.

The first section of this report pertains to the data needed as input into the Steady-State Spectral WAVE Model (STWAVE) and the Navy Standard Surf Model (NSSM). These inputs include wind forcing from the Coupled Ocean Atmosphere Mesoscale Prediction System (COAMPS), a high-resolution bathymetry (hypsography), and spectra from the Regional Wave Model (WAM), which describe the energy distribution in both the directional and frequency domains. Section 2.0 presents an overview of the STWAVE model, a description of the modeling procedure, and Sec. 2.4 discusses sample results for Camp Pendleton. This section concludes with cautions and conclusions. Section 3.0 describes the NSSM modeling procedure and sample results and Sec. 4.0 discusses issues that arose during the JDSZEM FY96 effort. Finally, Sec. 5.0 summarizes this documented effort.

1.1 COAMPS Wind Forcing

The wind input to all the numerical models discussed in this report were provided by COAMPS. Developed by the Naval Research Laboratory in Monterey, CA (Hodur 1993), COAMPS is designed

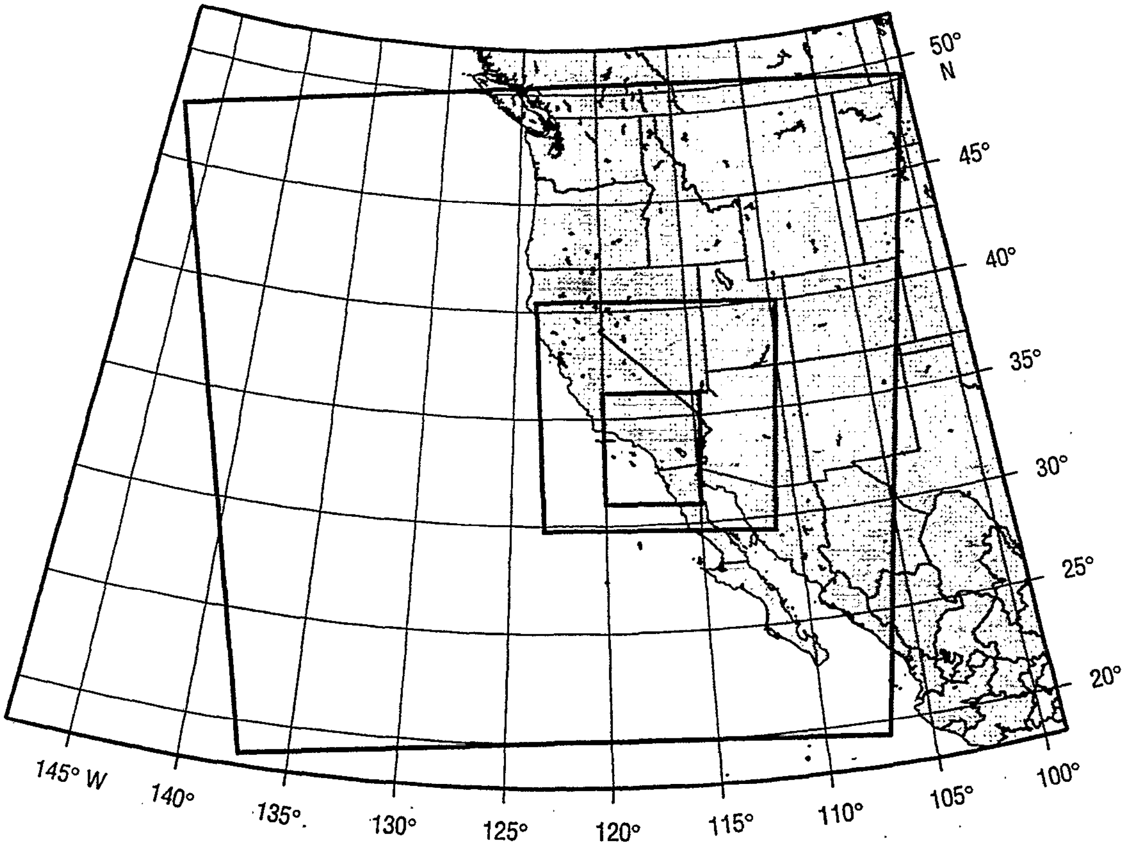

Fig. 1 — COAMPS triple-nested grid with resolutions of 45/15/5 km

to couple a nonhydrostatic, fully compressible atmospheric model to a hydrostatic, incompressible multilevel ocean model. The atmospheric model includes predictive equations for the momentum, nondimensional pressure perturbation, potential temperature, and mixing ratios of water vapor, clouds, rain, ice, and snow. Although the oceanic model is not included in the current version of COAMPS, the surface fluxes of momentum, heat, and moisture are parameterized and computed based on static oceanic fields.

The domain for COAMPS consists of a triple-nested grid, as shown in Fig. 1. While this grid has a 45/15/5-km mesh, the operational version of COAMPS will have a 81/27/9-km mesh. A COAMPS model run consists of an analysis step followed by a forecast run of user-specified length. For the analysis step, all available observations of wind conditions are blended with modeled data from the Navy Operational Global Atmospheric Prediction System (NOGAPS). This provides the initial guess field for COAMPS. Subsequent COAMPS runs obtain an initial guess field from the 12-h forecast of the previous run. All observations are taken from the Fleet Numerical Meteorology and Oceanography Command (FNMOC) operational data base and are quality controlled prior to use by COAMPS. Time-dependent boundary conditions for the inner meshes are provided by the next outer mesh.

A series of *special* COAMPS runs were performed in support of the MEL Integrated Synthetic Scenario Task (Allard 1996). COAMPS was run at 3-h increments for two 2-wk periods: 2 Jan 1995 00Z to 16 Jan 1995 12Z and 11 Aug 1995 00Z to 25 Aug 00Z. Figure 2 depicts the 10-m surface

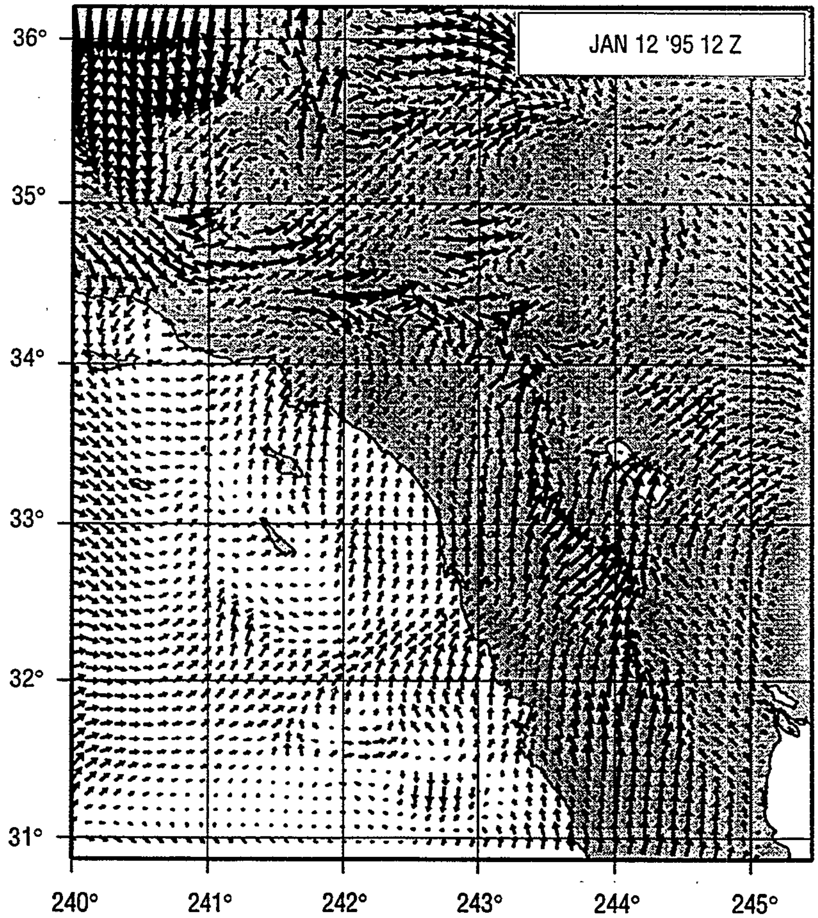

Fig. 2 — COAMPS 10-m wind field on the 5-km inner-mesh grid for 12 Jan 1995 12 Z

wind field over the entire 5-km COAMPS domain for 12 Jan 1995 12Z. Every other gridpoint is shown. Figure 3 shows the COAMPS wind speed and direction for the innermost nested gridpoint near Camp Pendleton (33.28° N, 117.60° W) for the January and August 1995 time periods, respectively. The plotted winds were used as inputs to both STWAVE and NSSM.

1.2 WAM Wave Model

The wave model in this study is the WAM spectral wave prediction model developed by the WAMDI Group (1988; also Komen et al. 1994), an international consortium of wave modelers. WAM describes the sea surface as a discretized, 2-D (frequency and direction) spectrum of sea surface elevation variance density. For this study, the frequency is discretized into 25 bands with center frequencies ranging from 1/30 Hz to 0.32832 Hz, each frequency being 1.1 times that of the next lower band. Direction is discretized into 24 bands of width 15°. WAM computes the variance density in each spectral component. Energy is also propagated in space, with refraction due to depth variation and dispersion due to the nature of the waves.

WAM is run operationally by FNMOC and the Naval Oceanographic Office (NAVOCEANO). In addition to the global WAM, which is run at both FNMOC and NAVOCEANO (and provides

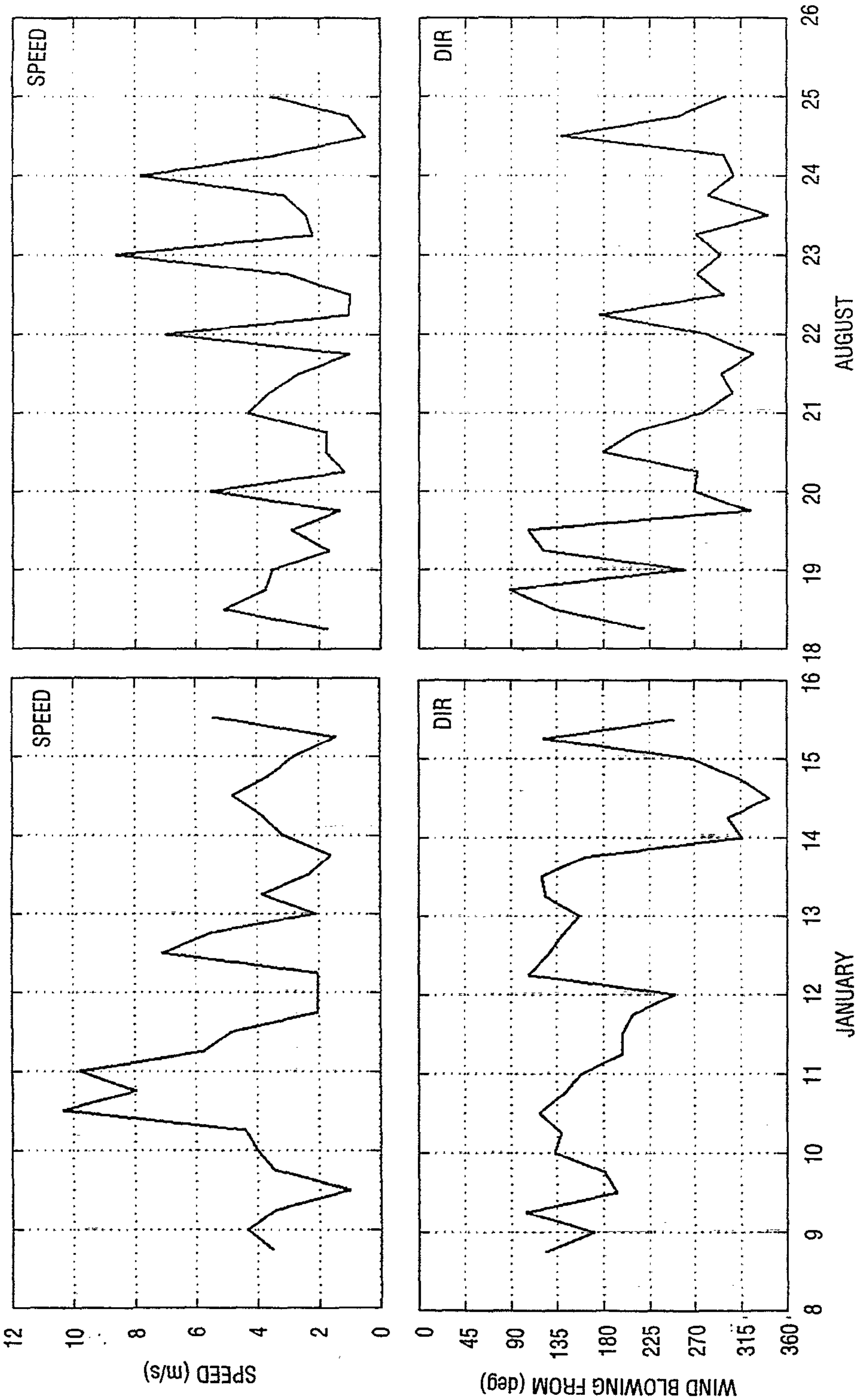

Fig. 3 — COAMPS wind speed and direction for January and August 1995 at 33.28° N, 117.60° W

boundary conditions for the regional WAM model runs), FNMOC and NAVOCEANO run WAM on a regular basis for the regions shown in Fig. 4. The rectangular boxes with a solid outline depict NAVOCEANO regional WAM domains; the dashed outlines represent FNMOC operational domains. Typical resolutions for these operational models range from 0.05° to 0.2°, with forecasts available in some instances out to 96 h.

For this particular study, JDSZEM utilized the NAVOCEANO Southern California WAM model, whose output had already been made available in support of the MEL Integrated Synthetic Scenario Task. The model domain (Fig. 5) has a resolution of 0.05° from 31° to 36° N and 120° to 115° W. This falls within the domain of the innermost COAMPS 5-km grid. Since most of the wave energy propagates into the grid from regions of the Pacific outside the grid boundaries, the grid is nested within a 1° global grid. For the inner grid, COAMPS is used for wind input, while the NOGAPS global wind field is used for the global WAM grid. Outputs saved from the high-resolution grid include: full spectra at selected points (see Fig. 5), significant wave height, average frequency and direction, sea and swell height, and frequency and direction at all water points. Appendix A shows a sample WAM spectral file for 12 Jan 1995 at 12Z. The entry on the first line represents the initial frequency (shown in bold) of 0.03333 Hz. The following five lines depict the energy distribution (m^2/Hz/rad) for each of the 24 directional bands *(centered at: 0, 15, 30, 45, 60, 75, 90, 105, 120, 135, 150, 165, 180, 195, 210, 225, 240, 255, 270, 285, 300, 315, 330, and 345°).* This procedure is repeated for the remaining 24 frequencies; however, only the first and last three frequencies are shown for brevity.

Figure 6 shows a comparison of the significant wave height between (1) 1.25° global WAM, (2) 0.05° Southern California regional WAM, and (3) buoys 46045 and 46054 during the period of 8–14 Jan 1995. One can see that the regional WAM model shows better agreement with the buoys than the global WAM output. The global WAM data were only available at 12-h intervals and were interpolated to the buoy locations. Quality-controlled buoy data were available on an hourly basis compared to 3-hourly for the regional WAM model. The buoys show much more variability due in part to the response to the actual wind field; however, the regional WAM model accurately shows

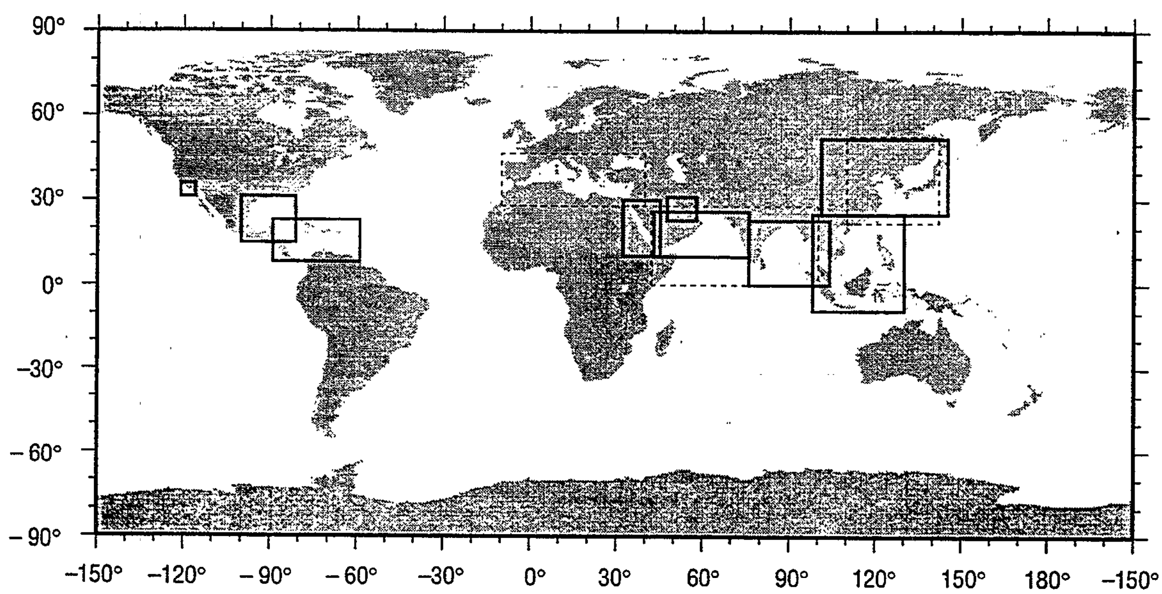

Fig. 4 — NAVOCEANO (solid rectangle) and FNMOC (dashed rectangle) regional WAM operational domains

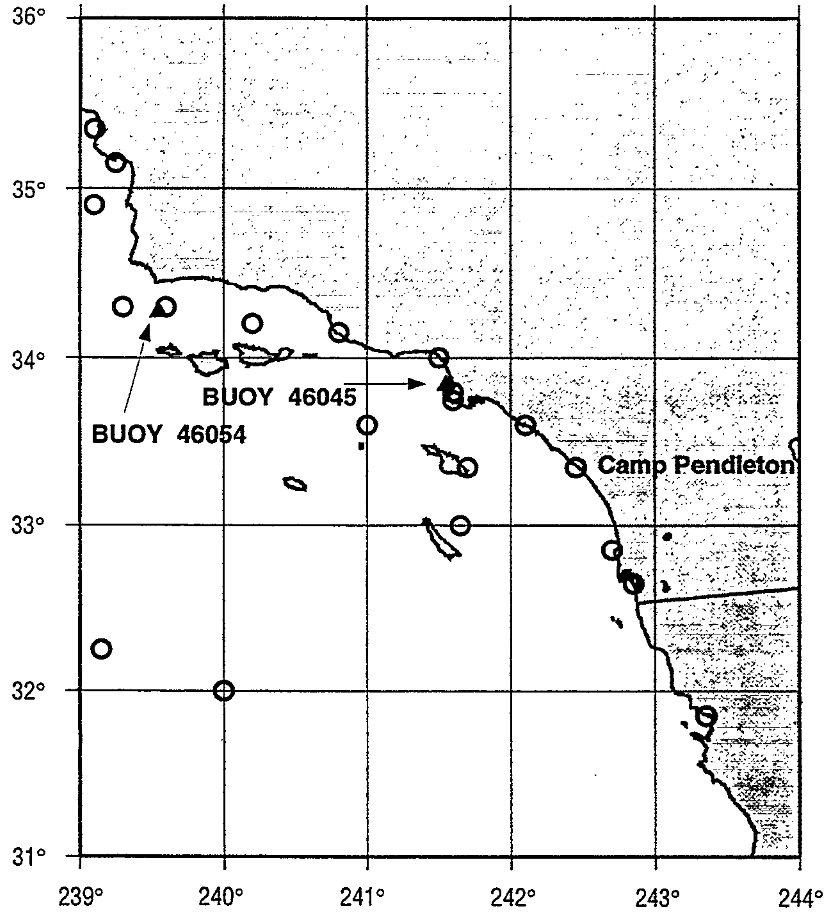

Fig. 5 — Southern California regional WAM domain. Model resolution is 0.05°; open circles denote locations where WAM spectra were saved; solid triangles denote buoy locations.

the trends for both buoys. Figure 7 depicts a color Vis5D depiction of the entire WAM domain for 18 Aug 1995 00Z. The significant wave heights are highest (~2.6 m) well offshore and to the northwest of Camp Pendleton. Note the shadow effects on the lee side of the islands off the California coast. In this case, the islands block the wave energy from propagating around the islands.

WAM spectra were saved for 20 locations (Fig. 5). Spectra were available at 6-h intervals from 8 Jan 1995 18Z to 15 Jan 1995 12Z and 18 Aug 1995 06Z to 25 Aug 1995 00Z. However, only the spectra saved near Camp Pendleton (33.35° N, 117.55° W) were used for this study. The Camp Pendleton WAM spectra location was revised (Fig. 10) to 33.28° N, 117.606° W, 5.17 nmi downslope of the original location for the spectrum to originate in deeper water. Since WAM was run assuming a deep-water environment, shifting the spectrum was deemed acceptable considering the small displacement involved. The water depth at the original location was less than 10 m; the water depth at the revised location is approximately 300 m. Therefore, the WAM spectrum location was shifted from the surf zone to the refraction zone.

An example of the Camp Pendleton WAM spectra is shown in Fig. 8 for 2 days, 11 and 15 Jan 1995. The vertical axis represents *direction toward* in degrees (90° represents toward the east, 0° is toward the north) and the horizontal axis represents frequency in hertz. Logically, waves come in from the ocean, not land, and may be blocked by nearby islands. Therefore, the waves for this area should be going *toward* directions between north and east and *from* south and west. The

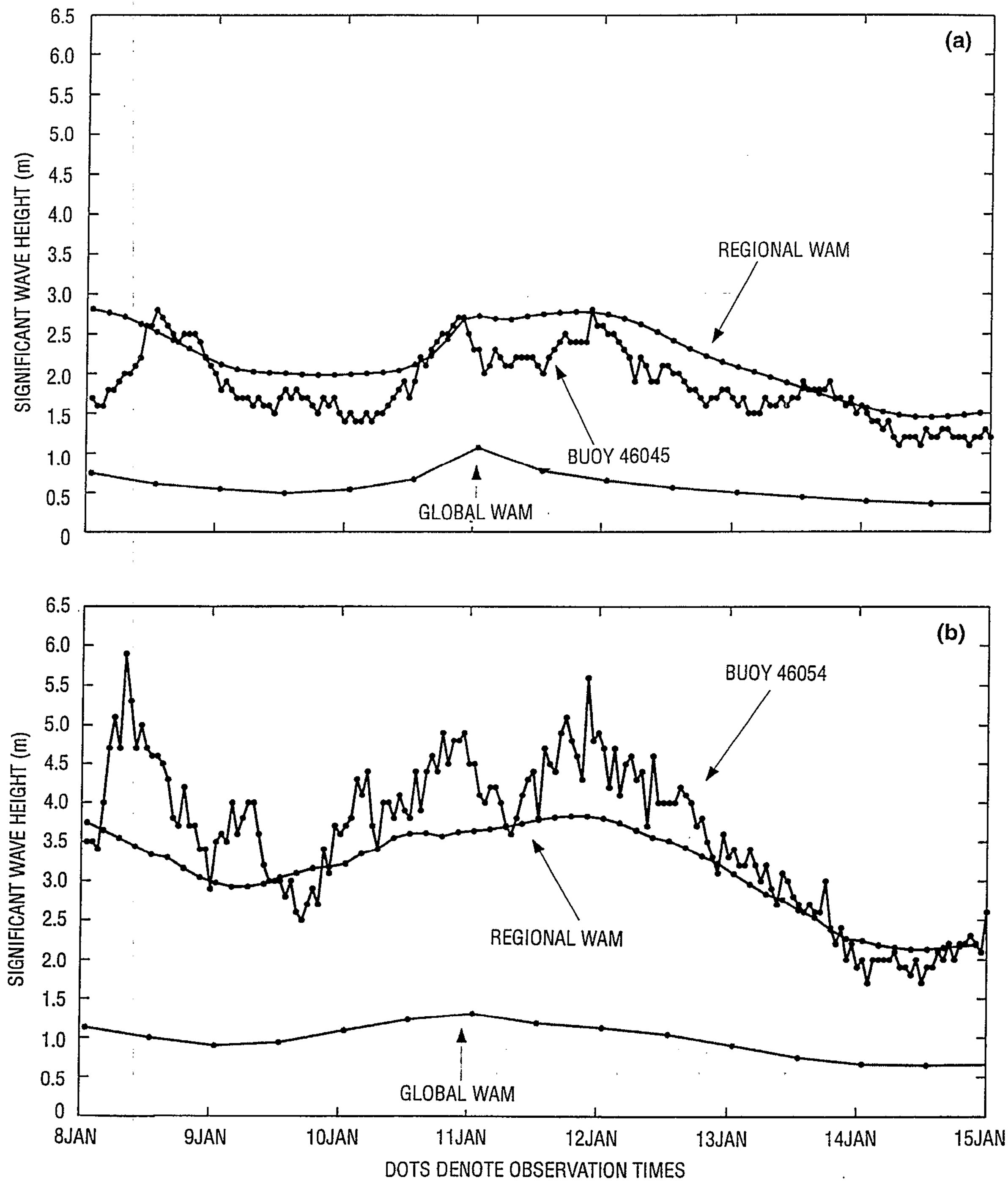

Fig. 6 — Comparison of significant wave height for 1.25° global WAM (12-hourly), regional WAM (6-hourly), and NDBC (hourly), (a) 33.84° N, −118.45° E and (b) 34.27° N, −120.45° E

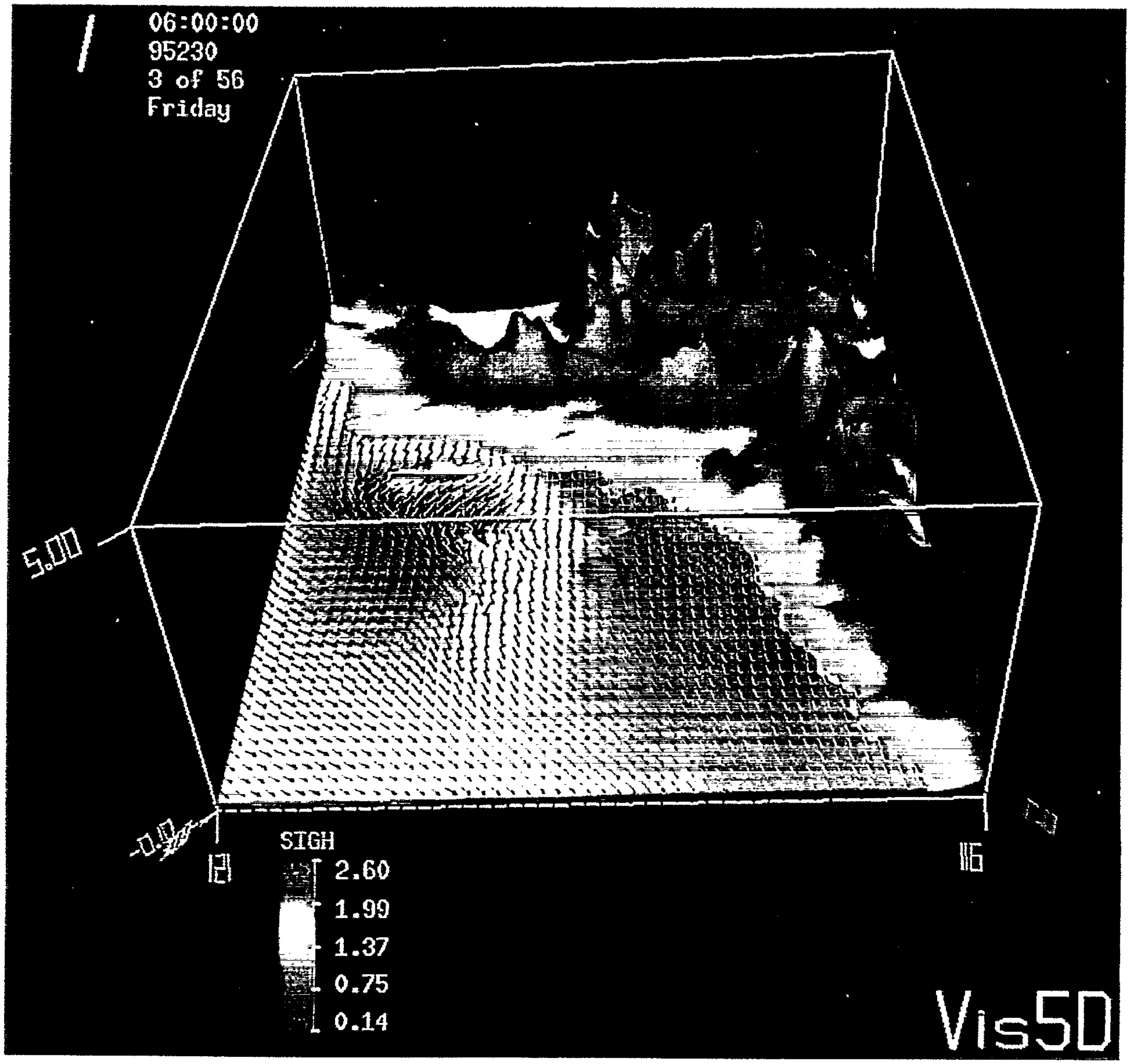

Fig. 7 — Vis5D depiction of WAM significant wave height for 18 Aug 1995

WAM spectra shown in Fig. 8 are consistent with these expectations. The high energy peak present from 11–15 Jan is due in part to a storm that affected the area.

1.3 Hypsography

The geographic area specified for the SE4 Demonstration was a 40-km square with the southwest corner at 439,000 and 3,669,000 in Universal Tranverse Mercator coordinates for Zone 9. This corresponds to geographic limits of 33.16° to 33.52° N and 117.65° to 117.22° W. The hypsography data base covers a smaller geographic area with limits of 33.1862° to 33.357° N and 117.642° to 117.402° W. To put these two geographic areas into perspective, Fig. 9 shows the southern California coast with the SE4 geographic limits as the plotting limits. The rectangle at lower left indicates the

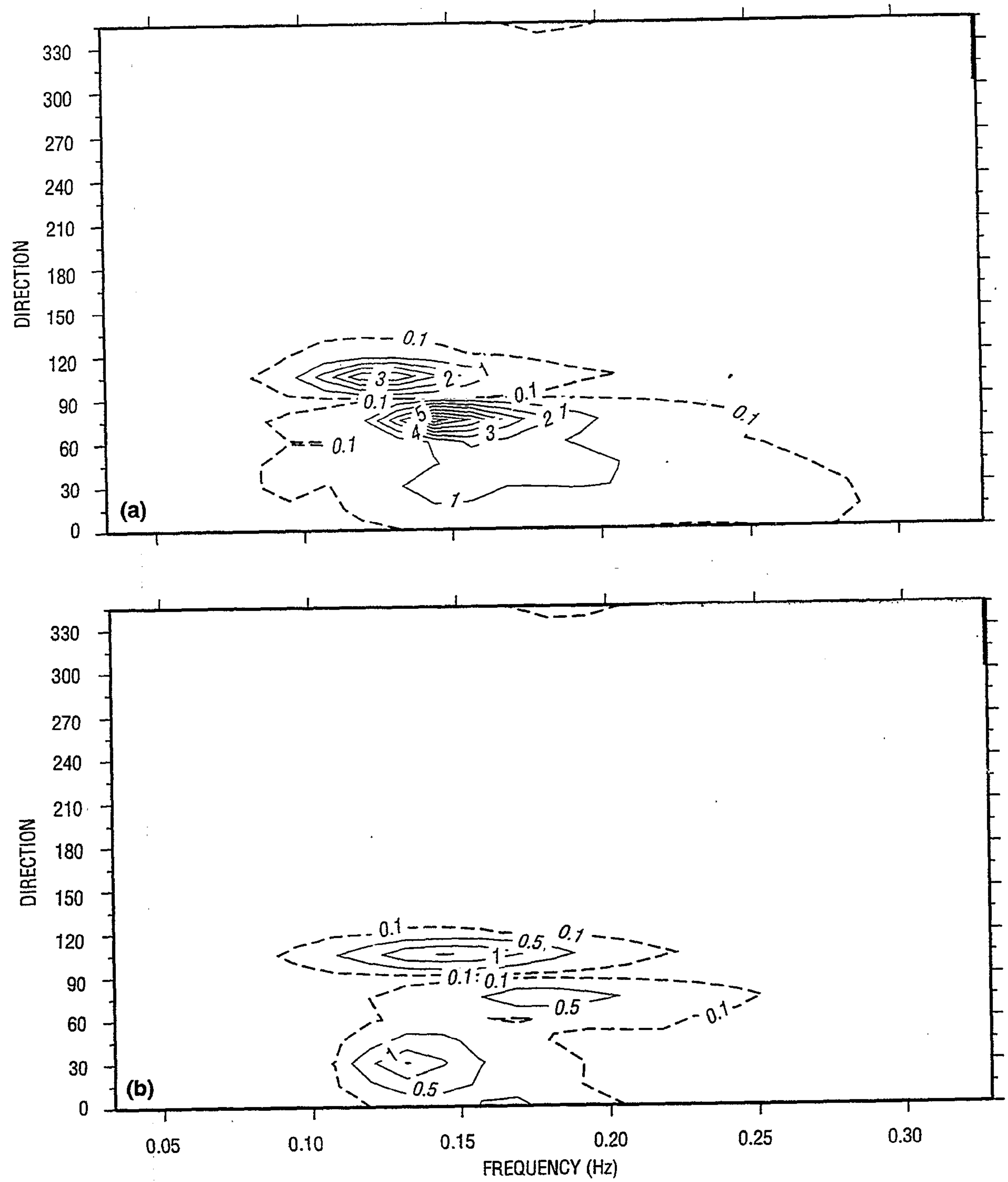

Fig. 8 — WAM spectra (Hz/m^2/rad) for (a) 11 Jan 1995 (solid line denotes contour interval of 1.0, dashed line represents 0.1 contour) and (b) 15 Jan 1995 (solid line denotes contour interval of 0.5, dashed line represents 0.1 contour)

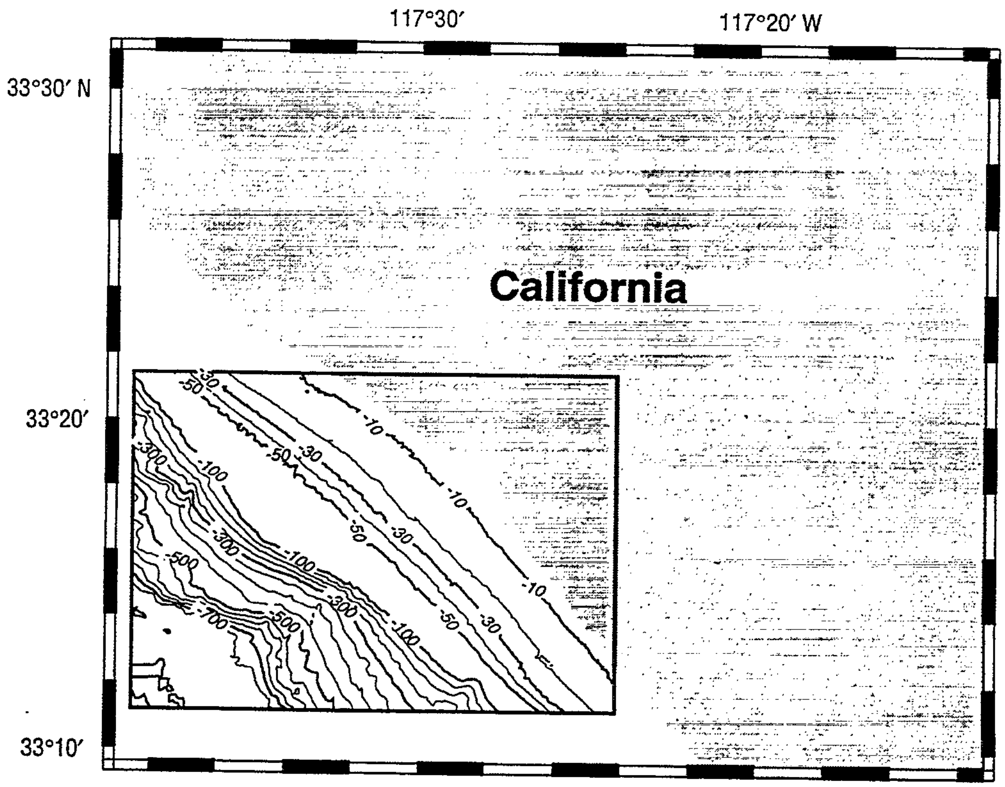

Fig. 9 — Southern California coast with inset Synthetic Environment 4 (SE4) demonstration area

hypsography data base's geographic limits. The bathymetric contour interval is 10 m for water depths less than or equal to 50 m and 50 m thereafter. Most of the SE4 area suitable for STWAVE and NSSM modeling is covered by the hypsography data base. Therefore, STWAVE and NSSM modeling were limited to the area covered by the data base.

The Camp Pendleton hypsographic data (provided by John Breckenridge of NRL) is based in part on raw National Ocean Service bathymetry. These data were regridded to a horizontal resolution of 100 m and are shown in Fig. 10. The red, white, and blue beaches labeled in Fig. 10 were considered during preliminary discussion for SE4 modeling, but were not directly modeled by STWAVE or NSSM. They provide geographic references for those familiar with the Camp Pendleton area. Also shown in Fig. 10 is the revised location of the WAM spectrum used for the STWAVE and NSSM modeling effort. As discussed previously, the revised WAM spectra location is in approximately 300 m of water. Fig. 10 also depicts the surf zone with 1-m depth resolution for the range from 10 to 1 m. Bathymetrically, the region is fairly benign in both the refraction and surf zones.

2.0 SURF ZONE WAVE MODELING

2.1 Introduction

The spectral wave transformation model STWAVE (Resio 1987, 1988a, 1988b; Davis 1992) was selected to transform offshore wave spectra that were hindcast using the WAM model (see

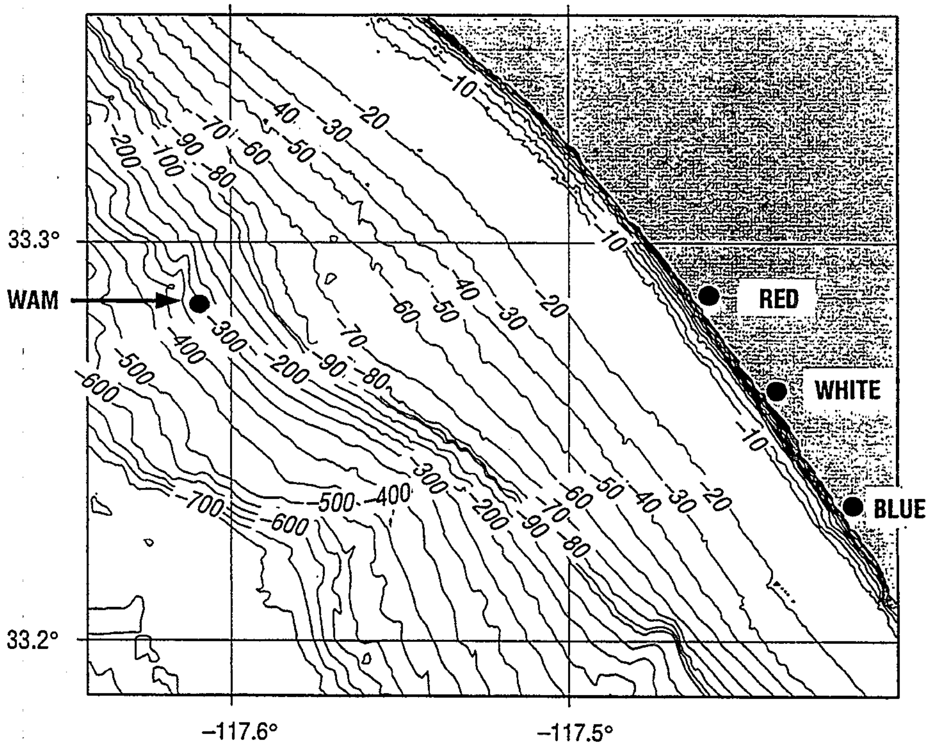

Fig. 10 — Camp Pendleton bathymetry used in JDSZEM modeling. Bathymetry has a horizontal resolution ($dx = dy$) of 100 m

Sec. 1.2) into the nearshore and surf zone to provide descriptions of the natural environment for joint exercises and deployments, including modeling and simulation activities. A spectral wave model was selected because it provides not only the wave height, period, and direction in the nearshore, but also the 2-D wave spectra (wave energy as a function of frequency and direction). The 2-D spectra can be used to construct realistic water surface representations for environmental simulations.

The purpose of this section is to document the procedure used to transform wave spectra into the surf zone. First, an overview of the STWAVE model is given. Next, the modeling procedure is described. Then sample results from STWAVE simulations at Camp Pendleton, CA, are described to illustrate the modeling results. This section ends with cautions and conclusions.

2.2 STWAVE Overview

The STWAVE model numerically solves the steady-state spectral energy balance equation

$$\frac{\partial C_{g_x} E(f,\theta)}{\partial x} + \frac{\partial C_{g_y} E(f,\theta)}{\partial y} = \sum S\,, \tag{1}$$

where E = spectral energy density, f = frequency of spectral component, θ = propagation direction of spectral component, C_g = group velocity of spectral component, x,y = spatial coordinates, and S = energy source/sink terms. The source terms include wind input, nonlinear wave-wave interactions, dissipation within the wave field, wave-bottom interactions, and surf zone breaking. The terms on the left side of Eq. (1) represent wave propagation (refraction and shoaling) and the source terms on the right side of Eq. (1) represent energy growth or decay in the spectrum. The assumptions made in STWAVE are:

- mild bottom slopes,
- negligible wave reflection,
- spatially homogeneous offshore wave conditions,
- steady wave and wind conditions, and
- linear refraction and shoaling.

STWAVE is a half-plane model, meaning that waves only propagate toward the coast. Waves reflected from the coast or waves generated by winds blowing offshore are neglected. Surf zone wave breaking limits the total wave height based on the local water depth.

STWAVE is a finite-difference model and calculates the wave spectra on a rectangular grid with square grid cells. The inputs required to execute STWAVE are:

- bathymetry and shoreline position,
- size and resolution of the grid,
- 2-D wave spectrum on the offshore grid boundary, and
- wind speed and direction.

The model outputs zero-moment wave height (H_{mo}), peak spectral period (T_p), and mean wave direction (θ_m) at all gridpoints and the 2-D spectrum at selected gridpoints.

2.3 Modeling Procedure for Camp Pendleton

The wave modeling procedure is presented to document how simulations were performed for Camp Pendleton and to document the procedure for future applications. The modeling procedure includes generation of the finite-difference grid, specification of model input parameters, waves and winds, and model execution.

2.3.1 Grid Generation

STWAVE operates on a flat grid with square grid cells. The optimal grid orientation is for the y axis to be aligned with the bathymetry contours and the x axis to be aligned normal to the contours. This orientations allows the greatest range of offshore wave angles and the most reliable modeling results. Bathymetry was supplied by NRL for the Camp Pendleton region for latitudes from 33.186° to 33.357° N and longitudes from –117.403° to –117.642° W. The resolution was approximately 100 m. To convert the bathymetry to a flat grid, the latitude-longitude references were converted to meters relative to the southwest corner of the original bathymetry (33.186° N, –117.642° W). Since the grid region was relatively small, constant conversions for the latitude and longitude were used. Following conversion of the bathymetry to metric coordinates, the southeast corner of the bathymetry was augmented, assuming straight-parallel bottom contours in that region (Fig. 11). The augmentation was required so that the grid could be aligned with the bottom contours. Next, the STWAVE grid was generated using the ACES2.0 URGG (Uniform Rectilinear Grid Graphical

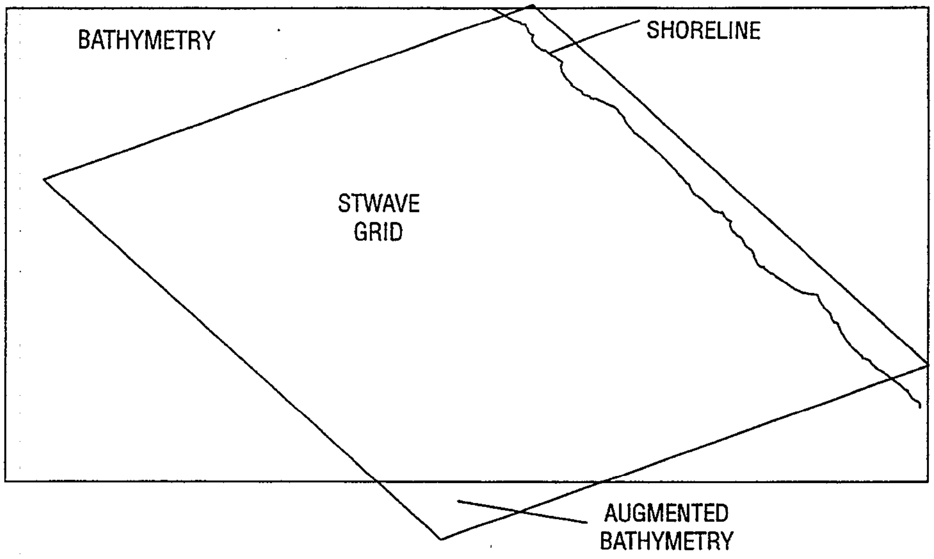

Fig. 11 — STWAVE grid orientation showing augmented bathymetry

User Interface software (Leenknecht and Tanner 1997). The orientation of the grid was selected to be 50° relative to north so the grid was aligned with the shoreline and bottom contours as shown in Fig. 11. For Camp Pendleton, the grid was specified as 121 cells in the cross-shore direction and 191 cells in the longshore direction, with a grid resolution of 100 m. URGG uses Delauney triangulation to develop the grid and linear interpolation to assign elevations at each cell. After generation of the grid, the seabed elevations (– values) were converted to depths (+ values) as required for STWAVE input. The grid depths were smoothed with a simple 5-point scheme.

2.3.2 *STWAVE Input*

STWAVE input includes an options file that specifies the grid, use of the wind source term, spectral resolution, and model output locations. Two additional input files containing the water depths for the grid and the input spectra are required to run STWAVE.

Options file. A truncated sample options file used for Camp Pendleton is given in App. B. The first line of the options file specifies the grid size (121 cross-shore grid cells and 191 longshore grid cells), the resolution of the 2-D spectra (25 frequency and 35 direction bands), the grid resolution (100 m), two binary switches for including the wind source (0 = include winds) and nondimensionalizing the spectra (0 = not nondimensionalizing), and the number of output points for which spectra will be saved (1856). Local wind forcing was used for all the Camp Pendleton runs. The 35 spectral direction bands correspond to a 5° directional resolution. The next three lines in the sample options file are the central frequencies for the 25 frequency bins. These frequencies were selected to match the WAM output spectra used to drive STWAVE. The remaining lines of the options file identify the I (cross-shore) and j (alongshore) indices of the STWAVE output points where spectra are saved. The depths corresponding to these gridpoints are given in the options file, but these are not used by the model. The $I = 1$ and $j = 1$ gridpoint is in the southwest corner of the grid.

Depth file. The depth file contains the depths for each gridpoint. This file was generated using the procedure described under grid generation.

Spectral input file. The main driver for the nearshore waves is wave spectra input on the offshore boundary of the STWAVE grid. These input spectra are the output from time-dependent WAM wave model runs, as discussed in Sec. 1.2. STWAVE is run with the same frequency resolution as WAM, but the STWAVE grid orientation and directional resolution differ from the WAM output. A 0° wave direction in WAM is a wave propagating to the north. In STWAVE, a 0° wave direction is propagating normal to the offshore edge of the grid. Thus, the WAM spectra were translated into the STWAVE orientation (STWAVE directions = 50° minus WAM directions). The directional coverage and resolution also differ between the WAM output and the STWAVE input. WAM spectra cover a full 360° with a resolution of 15°. STWAVE spectra cover a half plane (180°) with a resolution of 5°. WAM spectra were truncated to a half plane (neglecting waves traveling away from the coast) and the resolution was linearly interpolated from 15 to 5°.

Wind speed and direction are also input to STWAVE in the spectral input file. The wind parameters were supplied from COAMPS (see discussion in Sec. 1.1). The wind direction, like the wave direction, was translated into the STWAVE reference frame. The wind speed and direction were assumed constant over the STWAVE model domain.

2.3.3 STWAVE Execution

The wave and wind input to STWAVE come from time-dependent models. These models include temporal and spatial variations of the wave and wind fields over large spatial domains. Since the nearshore region of interest at Camp Pendleton is relatively small (20 km of beach), the time variation of the waves is modeled with a series of steady-state simulations. STWAVE was run at 6-h increments for two time periods: 8 Jan 1995 at 18Z to 15 Jan 1995 at 12Z; 18 August 1995 at 06Z to 25 August 1995 at 00Z. A total of 56 model runs were made. A steady-state wave model is much more computationally efficient than a time-dependent model for the fine grid resolution required in the nearshore. Depth changes due to the tide were not included in these simulations.

The model output includes the wave height (m), peak period (s), and mean direction (degrees relative to the STWAVE grid) for all gridpoints and the wave spectra (m^2/Hz/rad) for all gridpoints with depths less than 10 m. STWAVE was executed on the Cray YM-P at the Waterways Experiment Station. The application required 1 Mw of memory and less than 30 s CPU time. The spectra were saved for 1856 gridpoints for each model run. The output spectra for some of these locations were ingested into the MEL data base for easy access by the modeling and simulation community.

2.4 Camp Pendleton Sample Results

The previous section discussed the procedure used to apply STWAVE to calculate nearshore wave spectra at Camp Pendleton. This section shows sample results.

Figure 12 shows the depth contours over the STWAVE grid. The contours are in meters, with 0 m representing the shoreline. The x (cross-shore) and y (longshore) axes have been nondimensionalized, but their relative lengths are correct. Note that the foreshore slope is very gentle out to depths of about 100 m where the slope becomes relatively steep. In the lower left corner of the figure (the coastline is to the east (right)), the contour lines are unnaturally straight. This is the region where the depths were augmented assuming straight parallel contours. The offshore edge of the grid is deep water for all wave conditions. Since the bathymetry at Camp Pendleton is quite regular (straight-parallel contours), the wave transformation is fairly uniform along the shore. The dominant processes are wave shoaling, refraction, and surf zone breaking.

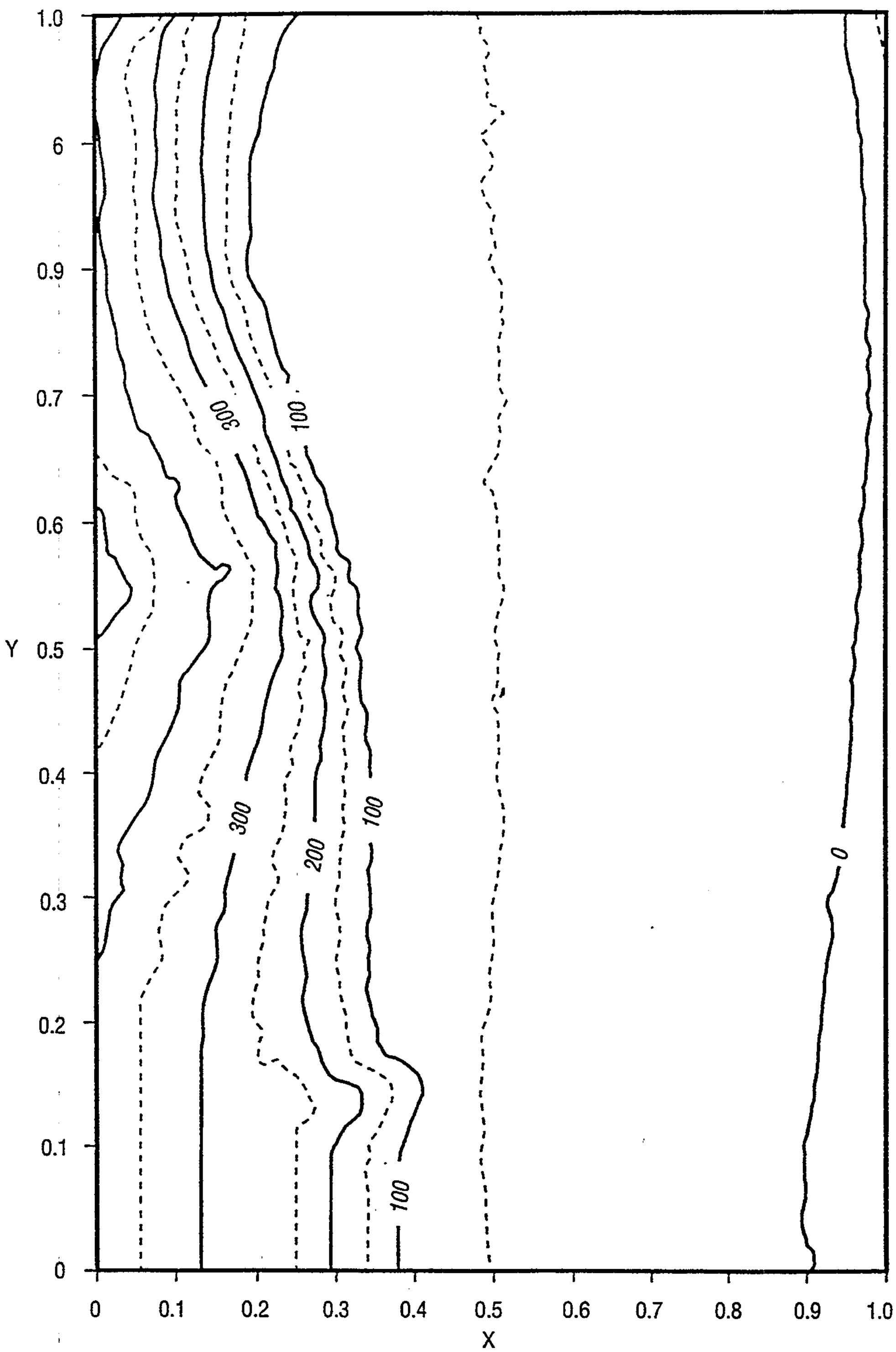

Fig. 12 — Camp Pendleton bathymetry used in STWAVE grid. Solid lines denote contours at 100-m intervals. The 0-m isobath represents the shoreline.

The waves during the January and August 1995 simulations are fairly typical of winter and summer conditions, respectively. The winter wave conditions are more energetic with wave heights of 1 to 2 m and peak periods of 12 to 15 s. The mean wave directions are coming from between southwest and west. Typical frequency and directional energy distributions from January 1995 are shown in Fig. 13 (from WAM). The directional distribution illustrates a problem with the WAM spectra. At 90° (waves from the west) the wave energy is blocked. This occurs in WAM when an island exists along a great circle path to the location of interest (see Fig. 7). The propagation scheme in WAM does not allow the wave energy to propagate "around" the island. This energy blocking impacts the nearshore transformation, but STWAVE propagates energy into this unrealistic dip in the energy distribution. Ignoring the anomalous dip in the direction distribution at 90°, there are two directional peaks (75° or WSW and 45° or SW) indicating that the waves are likely from two separate sources. The summer wave conditions are less energetic with wave heights of 0.5 to 1.1 m and peak periods of 4 to 15 s. The mean wave directions are coming from between south and west. Typical frequency and directional energy distributions from August 1995 are shown in Fig. 14 (from WAM). The spectra are relatively complex with multiple peaks in both frequency and direction. Note again the dip in the directional distribution at 90°. Also, note that the scale of the vertical axis changes between Figs. 13 and 14.

Figures 15–18 show transformed frequency and directional distributions of wave energy at four locations on the STWAVE grid (8 Jan 1995 at 18Z). The locations are given by the i and j indices in the upper right corner of the plots and represent a cross-shore transect at the central section of the beach. The local water depths for Figs. 15–18 are 9, 6, 3, and 1 m, respectively. The wave directions in Figs. 15–18 are relative to the STWAVE grid, so 0° is approximately SW, positive angles are more southerly, and negative angles are more northerly. The shape of the frequency spectra stays about constant for each location, but the energy level first increases as the depth decreases due to shoaling, and then the energy decreases due to wave breaking. The spectral shape stays constant because there is little or no additional wave growth between locations. The directional distribution of energy becomes narrower and more peaked in shallow depths. This is due to refraction turning the waves so they are more shore normal. Figure 19 shows contours of wave height for the same time period. The wave height increases due to shoaling and then decreases near the shoreline due to breaking. Figure 20 shows vectors of wave direction. Only every fourth gridpoint is plotted. As discussed before, the wave direction becomes nearly shore-normal near the shoreline.

Wind speed and direction impact wave transformation. The wind speeds at Camp Pendleton were significant (up to 10 m/s) during the simulation periods. The major impact of the wind was turning of the wave direction. Wave directions varied by as much as 30° including wind forcing. Had the grid covered a larger region, the wind may also have increased the wave energy significantly.

2.5 Cautions and Conclusions

The 2-D, steady-state, spectral wave transformation model STWAVE was used to transform WAM output into the surf zone. Use of a 2-D (x and y) model captures complex refraction patterns for regions of complex bathymetry, although the bathymetry at Camp Pendleton is fairly benign. Use of a spectral wave model preserves complex frequency and directional distributions in wave transformation (e.g., see Fig. 14). The output wave spectra provide information required to construct realistic water surfaces for environmental simulations, as well as wave height, period, and direction parameters.

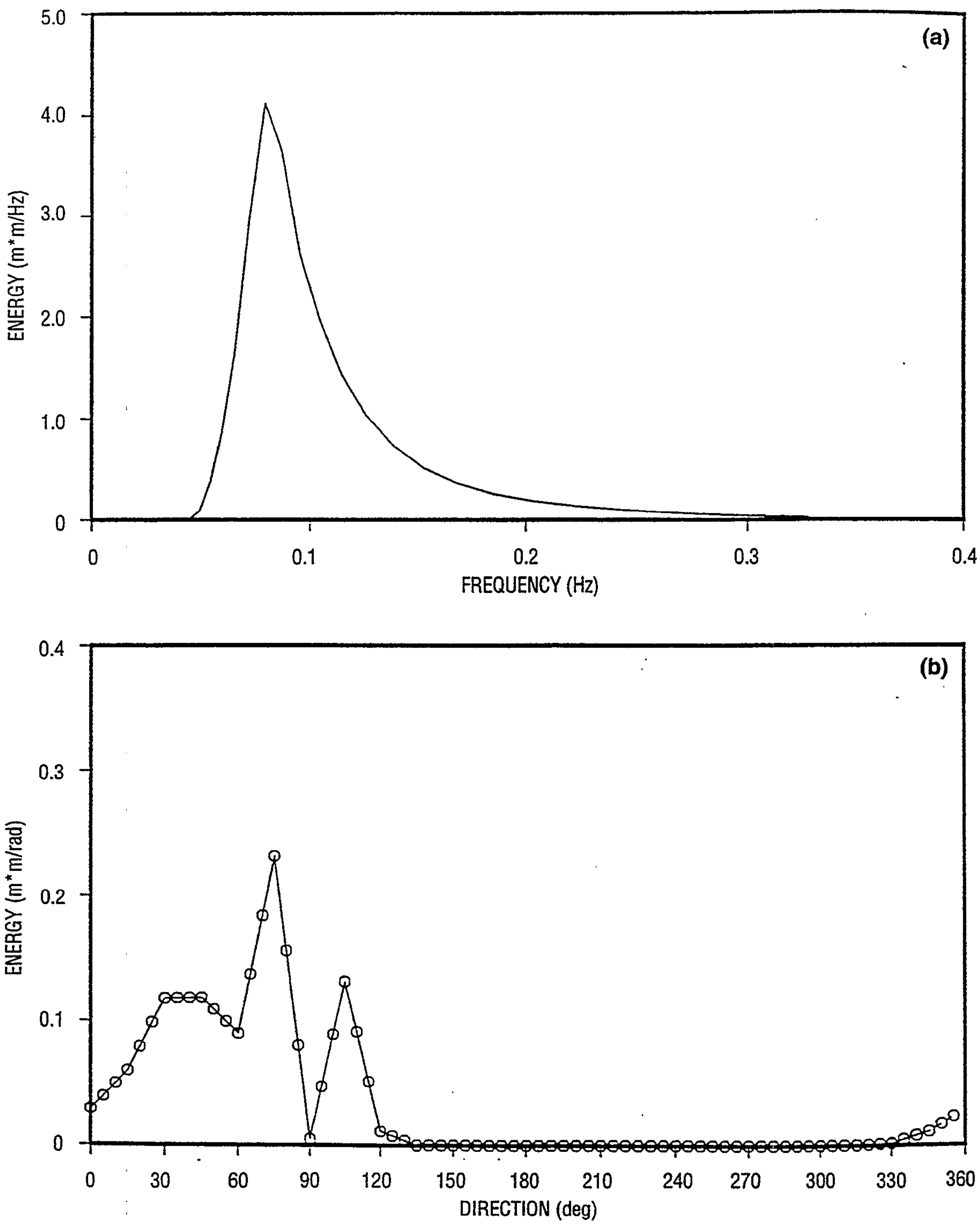

Fig. 13 — WAM distributions of wave energy for 8 Jan 1995, (a) frequency and (b) directional

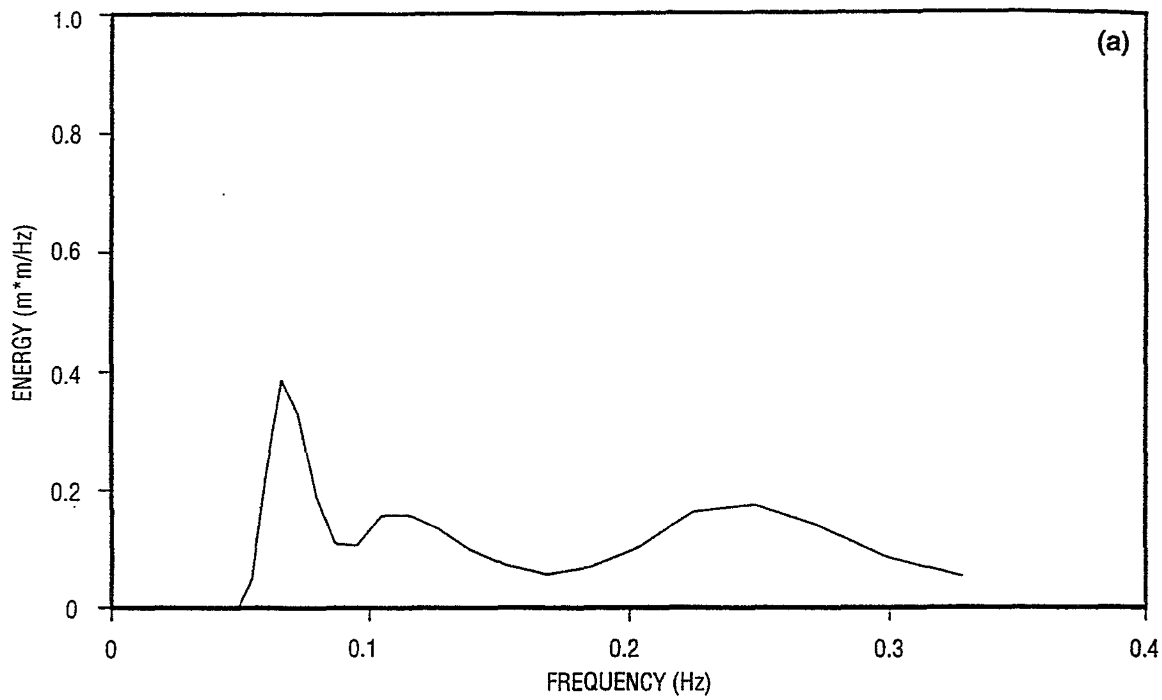

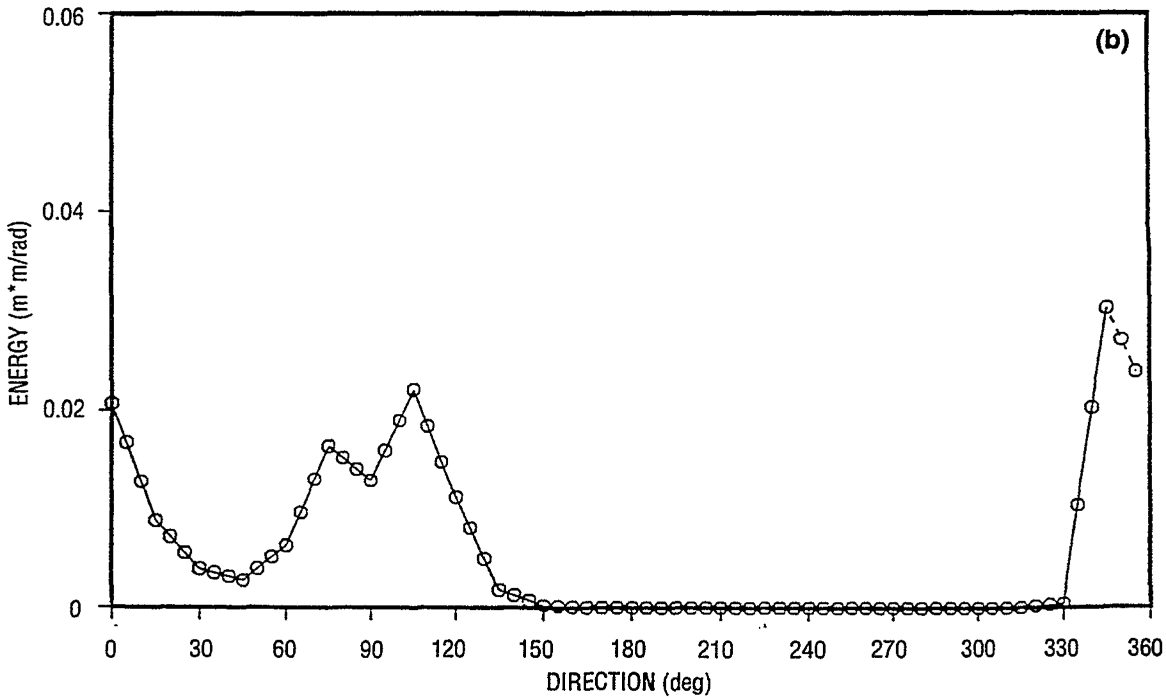

Fig. 14 — WAM distributions of wave energy for 22 Aug 1995, (a) frequency and (b) directional

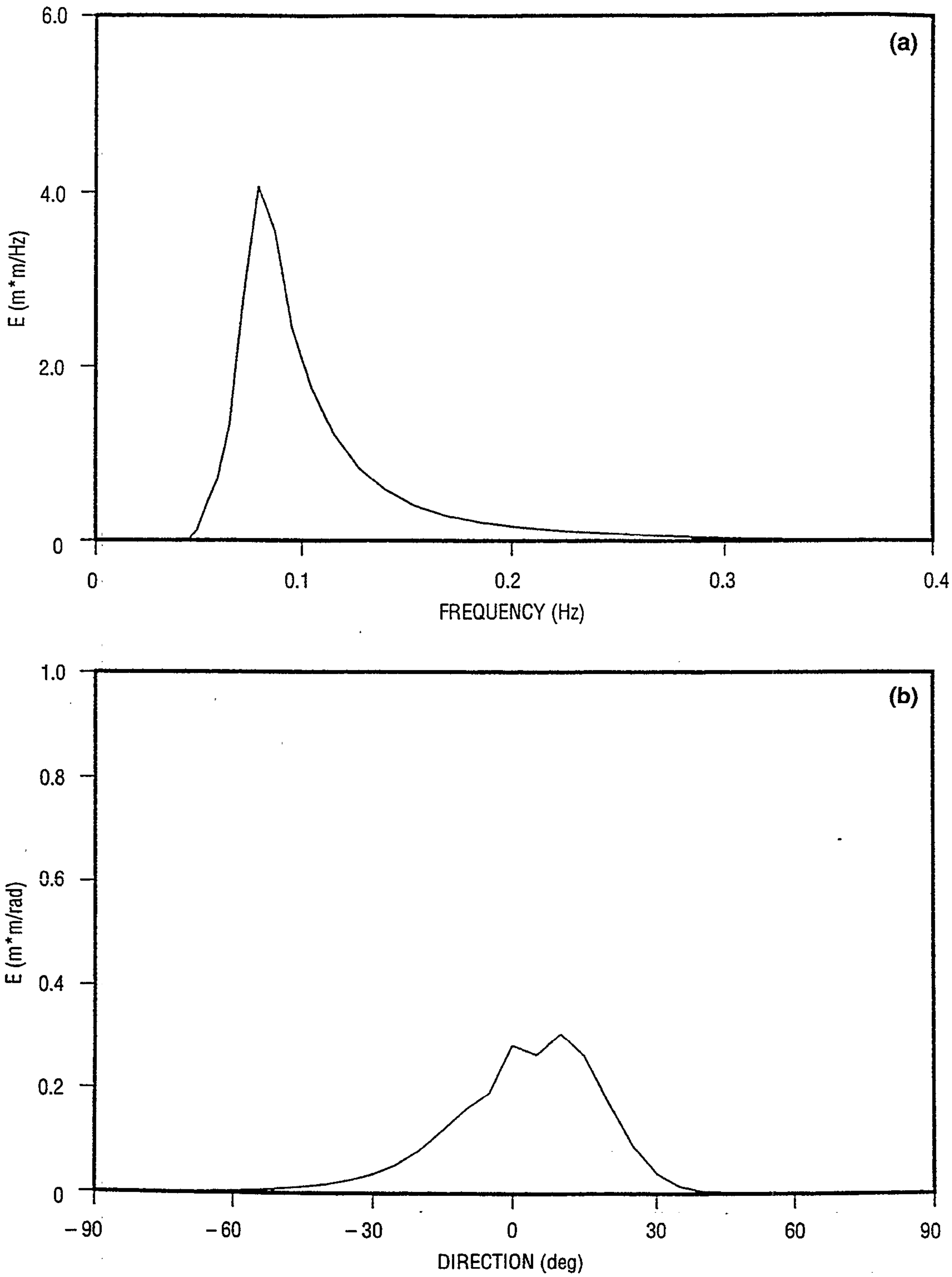

Fig. 15 — Transformed STWAVE distribution of energy at 9-m depth, (a) frequency and (b) directional

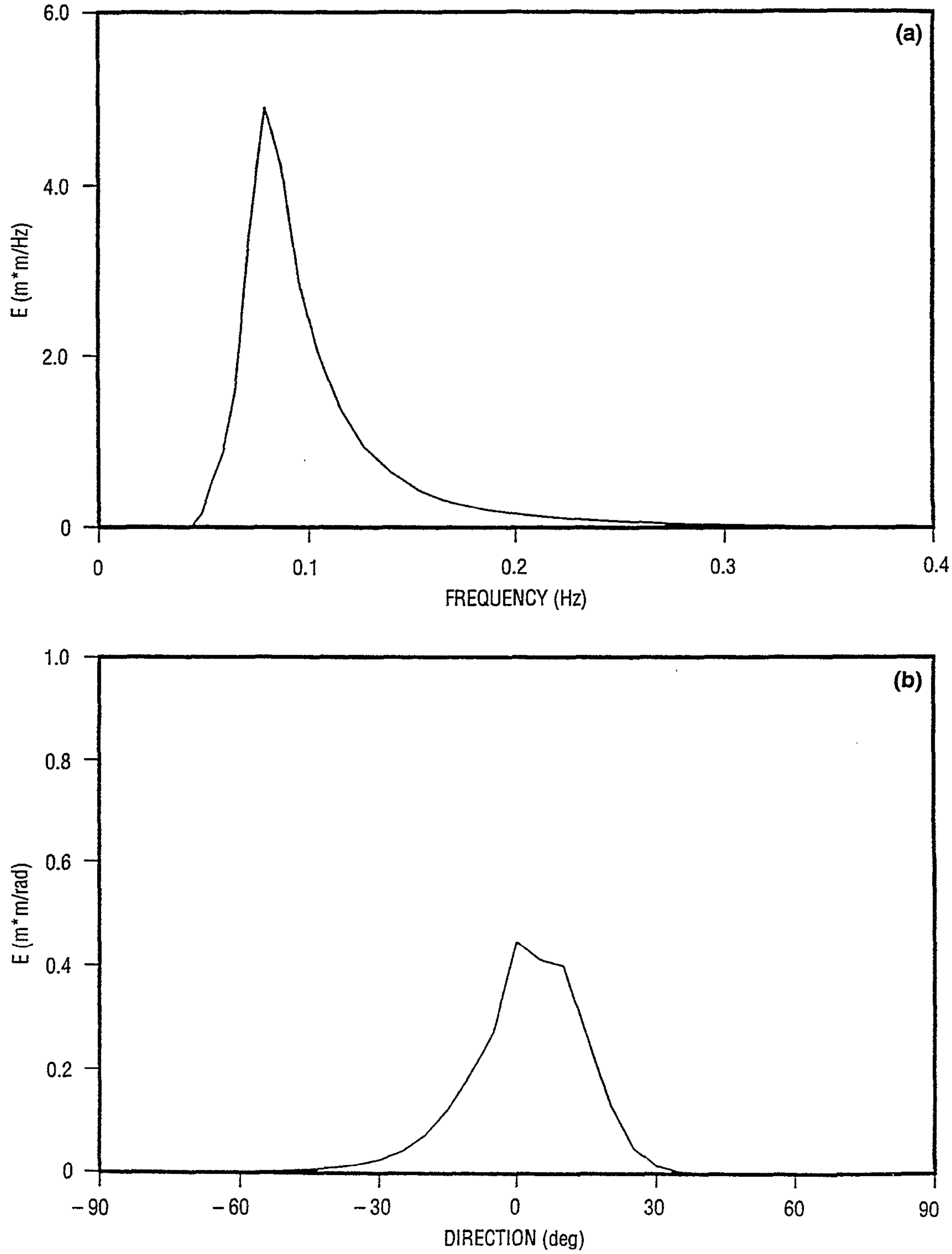

Fig. 16 — Same as Fig. 14, but for 6-m depth, (a) frequency and (b) directional

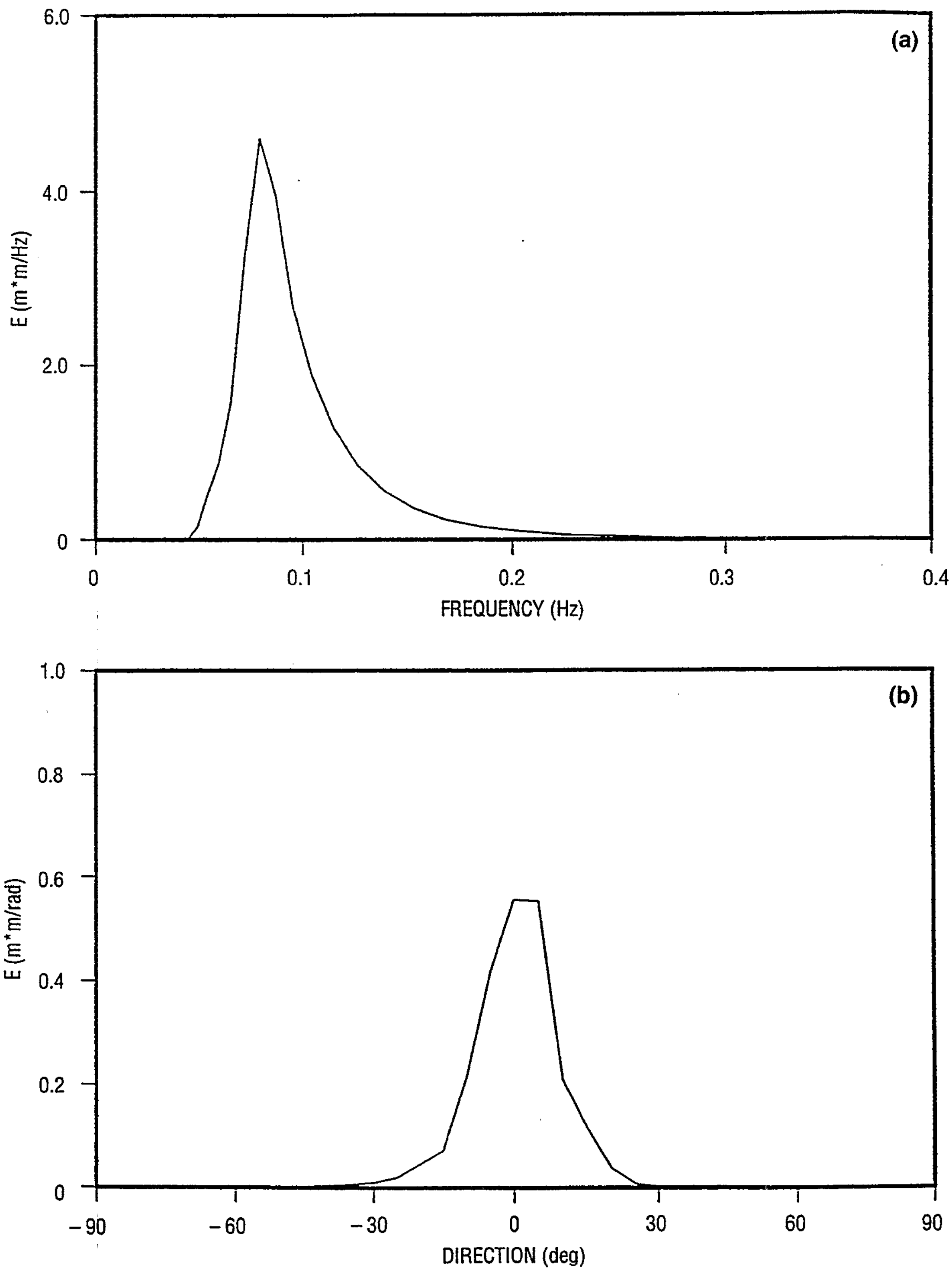

Fig. 17 — Same as Fig. 14, but for 3-m depth, (a) frequency and (b) directional

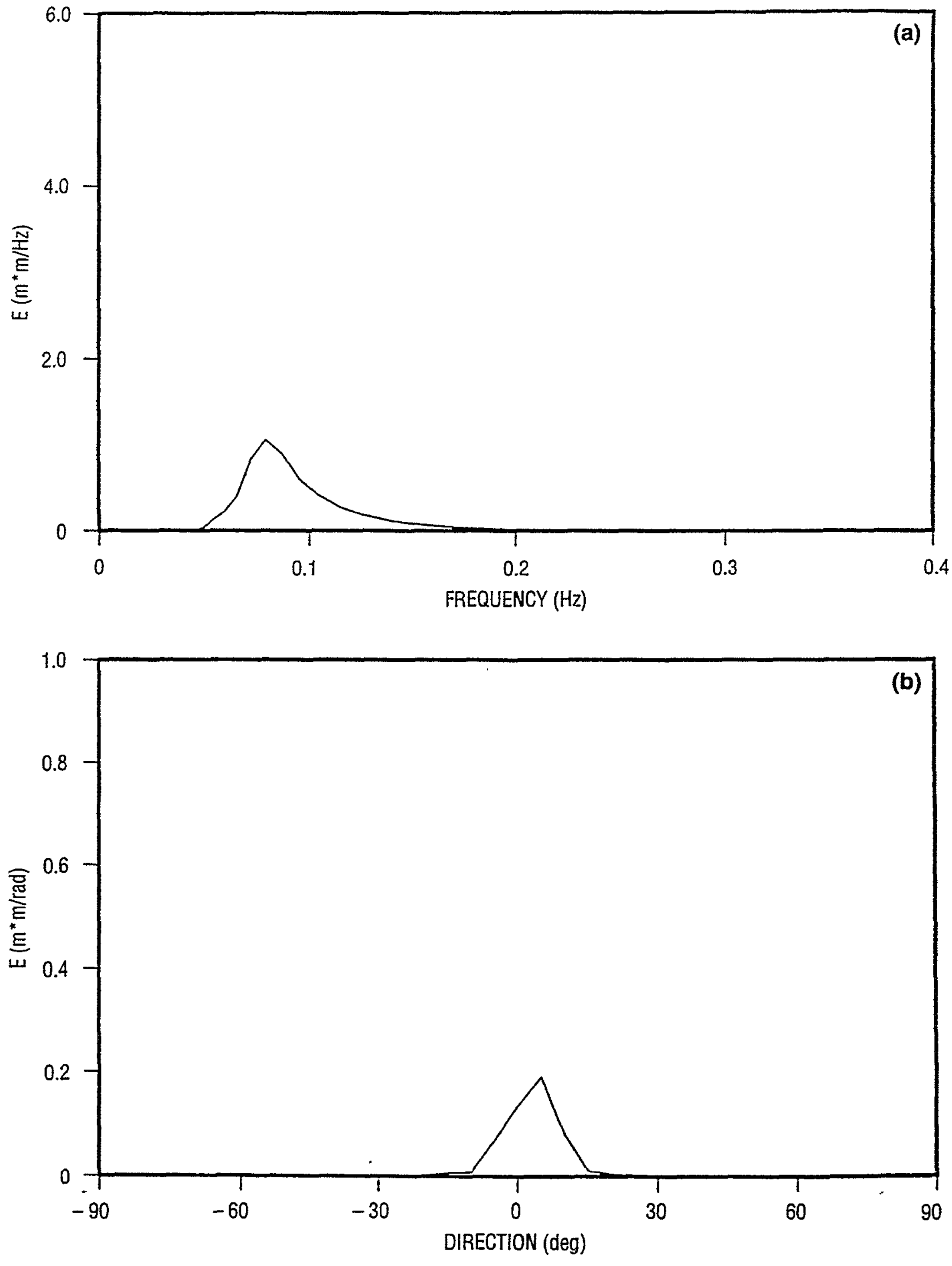

Fig. 18 — Same as Fig. 14, but for 1-m depth, (a) frequency and (b) directional

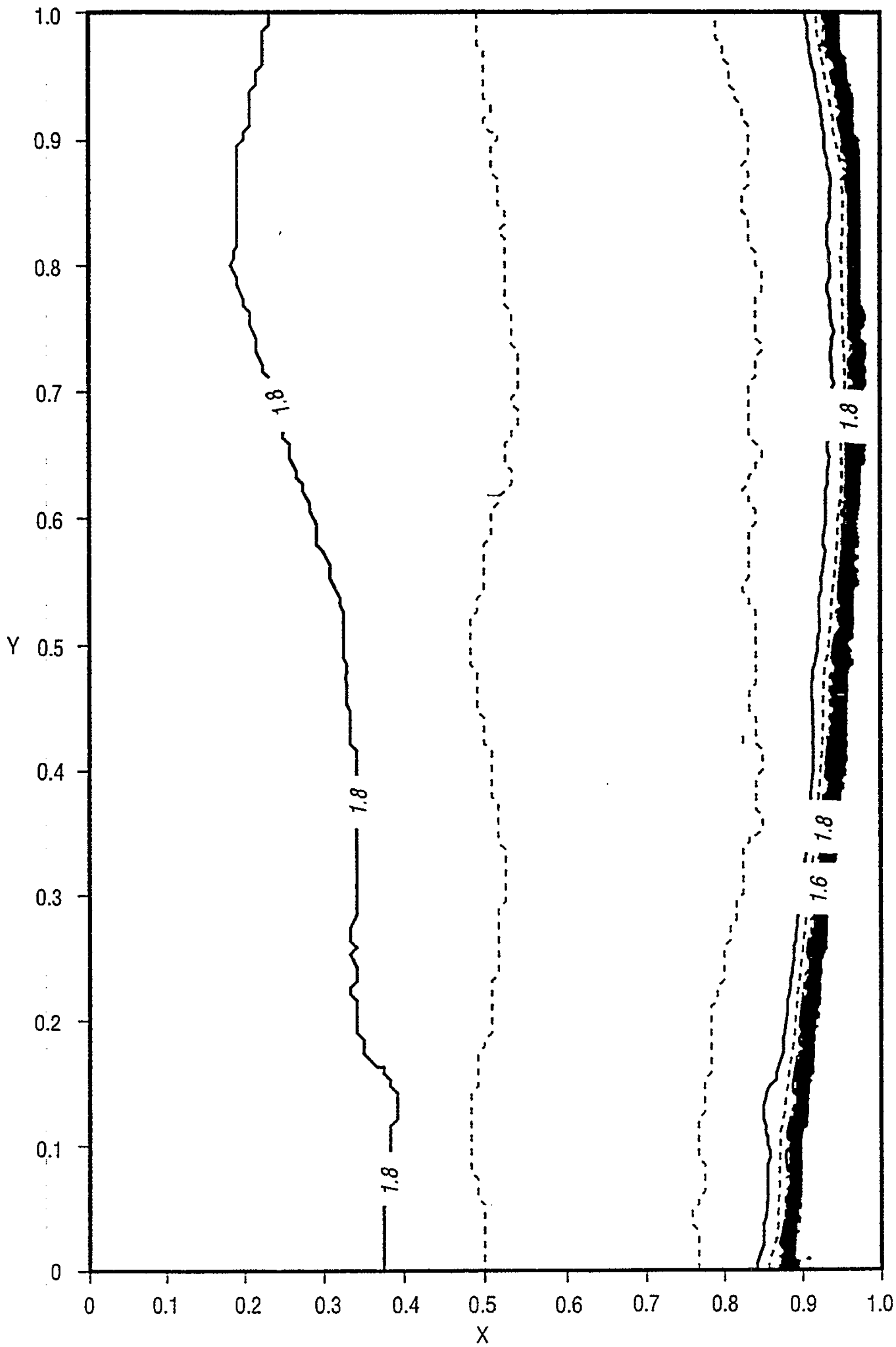

Fig. 19 — Wave height contours (m) for 8 Jan 1995 18Z

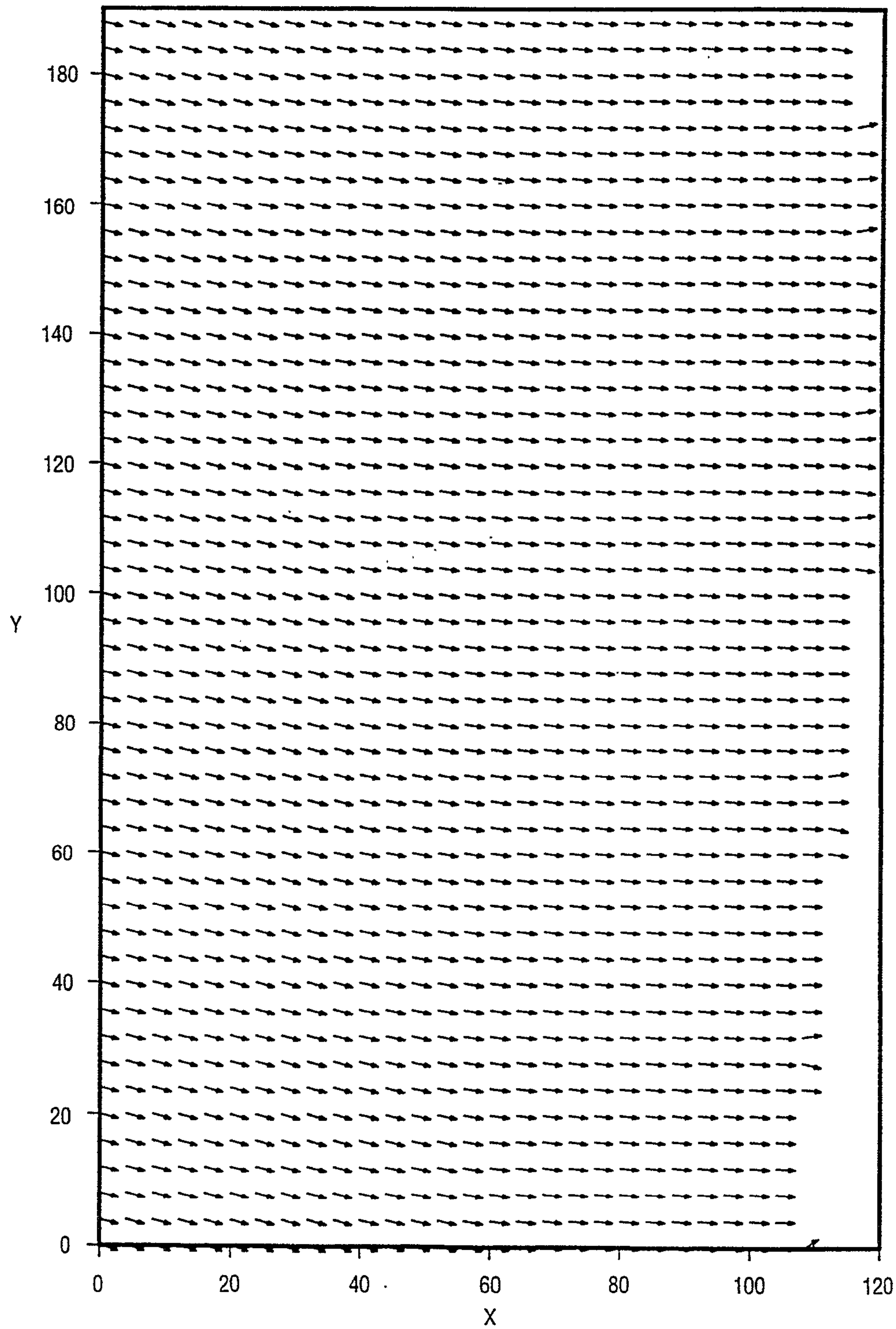

Fig. 20 — Wave direction vectors for 8 Jan 1995 18Z

The procedure for applying STWAVE is straightforward, but does require engineering judgment. The following cautions should be considered in future applications:

- As in any numerical modeling, the input and output of the model should be given a "reasonableness" test. For example, in the Camp Pendleton simulations, a problem was identified with the WAM spectra. Wave heights, periods, and directions should be reasonable (are heights reasonable for the local depth, are periods and directions reasonable for the possible fetches, etc.).
- Bathymetry must also be given a reasonableness test. The model assumes mild slopes, so extremely steep or rugged bathymetry may require smoothing.
- The grid orientation should be aligned as closely as possible with the bathymetry contours. Nonalignment with the contours will lead to waves traveling offshore (relative to the grid) and errors in the model.
- Although STWAVE includes the dominant processes for most applications, the processes of reflection, diffraction from a structure, wave-current interaction, and triad interactions (growth of harmonics) are not included. Also, for the Camp Pendleton simulations, depth changes due to the tide were neglected.
- STWAVE is a time-independent model. For wave simulations where the wave field changes rapidly (faster than the time for a wave to propagate through the grid), a time-dependent model should be considered.
- The spectral input into STWAVE is assumed constant along the offshore boundary. Thus, if the wave field differs significantly across the boundary, the model requires some alteration.

3.0 NAVY STANDARD SURF MODEL

Disclaimer: A version of NSSM that accepts WAM spectra as input was used for SE4 modeling. This FY96 version was developed for NRL by Neptune Sciences Inc. It is documented (Mettlach et al. 1996), but it is not the NSSM approved by Oceanographic and Atmospheric Master Library. The NSSM differences are in the acceptance of WAM spectra as input and the format of the ASCII output file. There are no differences in the physics.

The NSSM consists of two models, RCPWAVE and SURF (Earle, 1988, 1989, 1991; Mettlach et al. 1996). RCPWAVE is a wave refraction model developed by the U.S. Army Corps of Engineers Coastal Engineering Research Center. It uses finite-difference techniques to determine the effects of wave refraction as waves move from farther offshore into the surf zone. RCPWAVE includes wave diffraction and shoaling and is essentially an open coast model. Basically, RCPWAVE picks up where WAM leaves off, in deeper water, and models the waves until the surf zone is reached. In the surf zone, SURF models the wave characteristics and provides a surf forecast in the standard format specified in the *Joint Surf Manual* (1987).

NSSM input consists of a refraction zone depth grid, forecast date and time, landing zone name, starting depth, beach orientation relative to north, nearshore beach profile or linear beach slope, surf zone output interval, wind speed and direction, tide level, and wave spectra. If this version of NSSM (that accepts WAM spectra) had not been used, the sea wave height, period, and direction would have been needed.

NSSM outputs two different types of results, a surf forecast as specified in the *Joint Surf Manual* and a more detailed output. The surf forecast consists of significant and maximum breaker heights, dominant breaker period and direction, breaker type, maximum longshore current, typical number of breakers in the surf zone, width of the surf zone, and modified surf index. The detailed output (see App. C) is a function of distance offshore and consists of the water depth, significant and maximum breaker heights, percent breaking waves, wavelength, and longshore current.

For SE4, a refraction zone depth grid was built from the hypsography (Sec. 1.3) by determining the distance offshore versus water depth for equally spaced parallels to the beach approach. Using this crude refraction zone depth grid, RCPWAVE was run. Based on a statistical analysis of the surf zone hypsography and knowledge of NSSM's sensitivity to variations in beach slope, one landing zone with a linear beach slope of 0.007 was deemed sufficient to represent the Camp Pendleton surf zone. Once the tide level was determined from tide tables (NOAA 1995), SURF was run and NSSM's two-step modeling process was complete.

3.1 NSSM Output

Figures 21–25 show some of the NSSM output. The horizontal scale in Figs. 21–23 is the distance offshore in meters and the vertical scale is the date/time. The January time period is shown above the August time period. Figure 21 shows NSSM's modeled significant breaker height, which is defined as the average height of the one-third-highest breaking waves at a given location over a given time interval. In general, the significant breaker heights were higher for the January 1995 time period than for the August 1995 period. This was a result of the dominant winds being more from the open ocean for January than for August. In addition, the significant wave heights are higher for January as a result of distant winter storms. Two intense winter storms are responsible for the large significant breaker heights predicted during 9 and 12 Jan 1995. Referring to the WAM spectra displayed in Fig. 8 for 11 and 15 Jan 1995, the significant wave heights for 11 Jan should be and are higher than those for 15 Jan.

The percent breaking waves shown in Fig. 22 is the percentage of individual waves passing a given location that are breaking. The percent breaking waves are higher for January than August for the same reasons that the significant breaker height is higher in January than August; i.e., the dominant wind direction is more from the open ocean in January than August and distant winter storms increase the deep-water wave heights that subsequently cause higher surf conditions. The percent breaking waves for August are more variable in intensity as a function of time than for those for January. This is due to the wind speeds and directions for August being more variable than those for January.

Figure 23 shows the longshore current, the wave-induced current that moves parallel to the beach, with a positive value indicating a current moving to the right flank (toward the southeast) and a negative value indicating a current moving to the left flank (toward the northwest). For January, the dominant longshore current is toward the left flank, up the California Coast, with some strong wave-induced currents caused in part by the effects of distant winter storms. The longshore currents for August are smaller and more variable in intensity and direction.

Figures 24 and 25 show the surf zone width and the modified surf index, respectively, as a function of the date/time for both periods, January and August 1995. The width of the surf zone is defined as the distance from the beach to the farthest point where 10% of the waves are breaking. If 10% of the waves are not breaking at any location, the width of the surf zone is defined as the distance from the beach to the point where the most energy is lost due to breaking waves. A plot of the NSSM surf zone width is shown in Fig. 24. The surf zone width is greater for January than August.

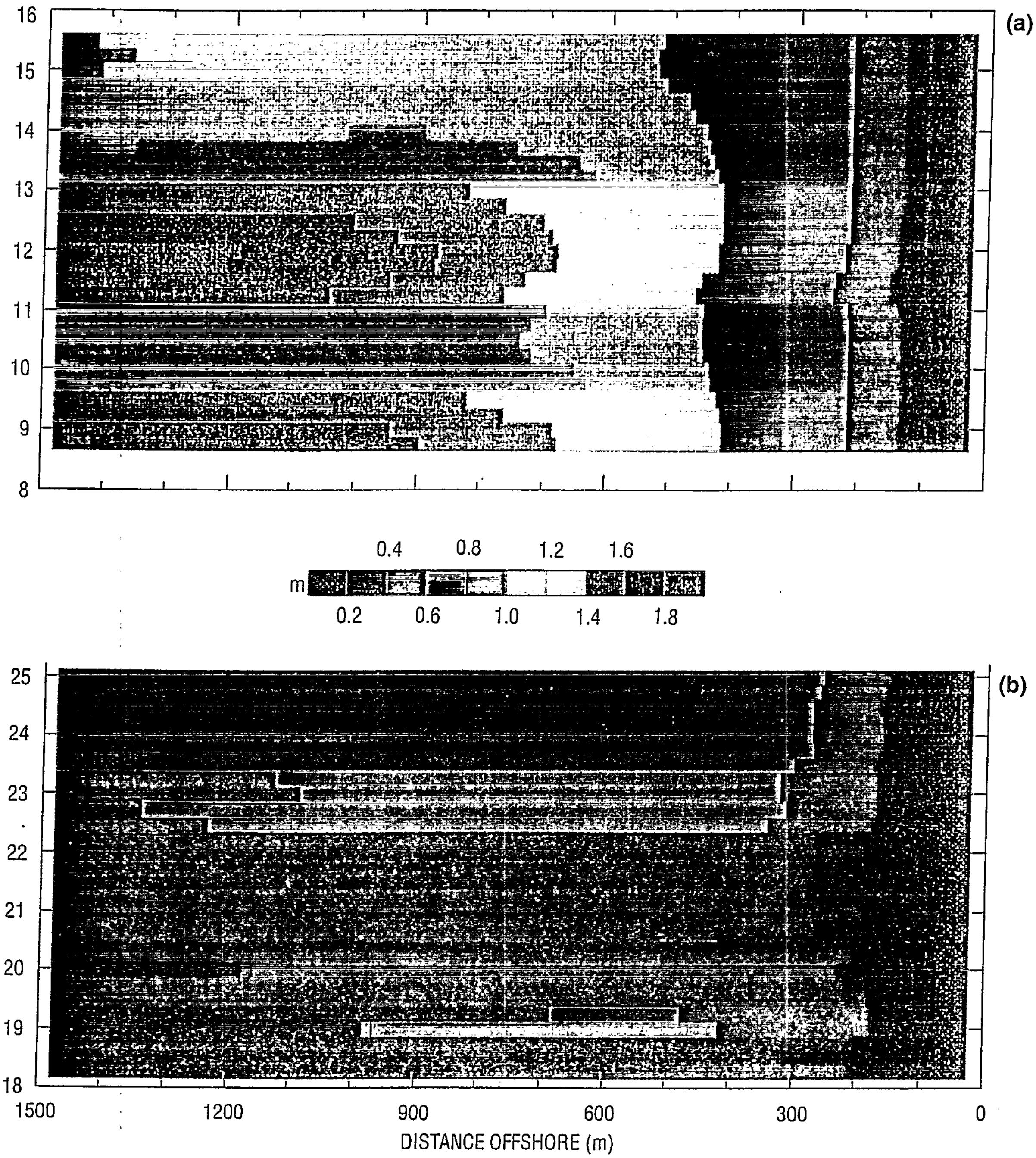

Fig. 21 — Navy Standard Surf Model (NSSM) significant breaker height for (a) January and (b) August 1995

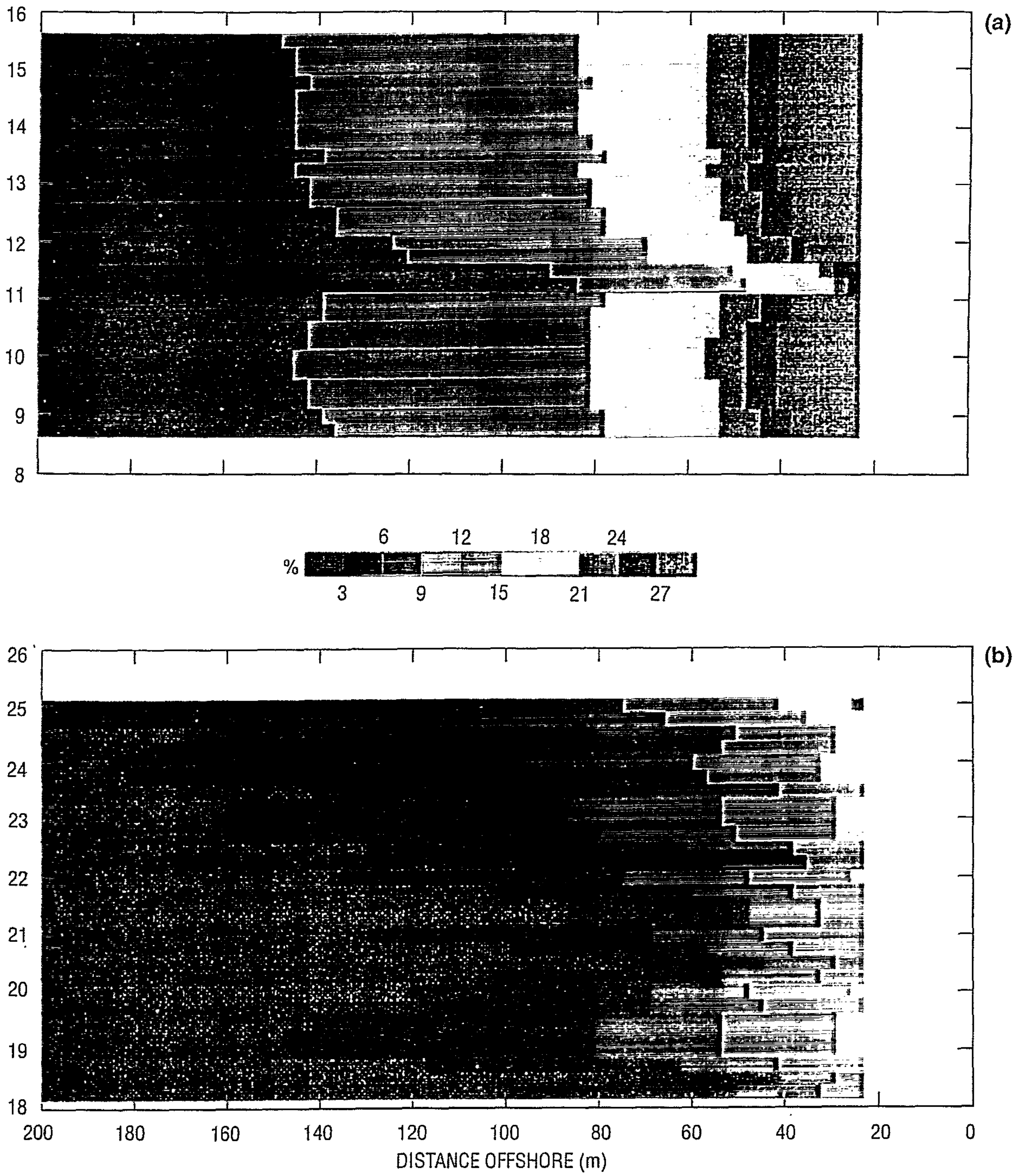

Fig. 22 — NSSM percent breaking waves for (a) January and (b) August 1995

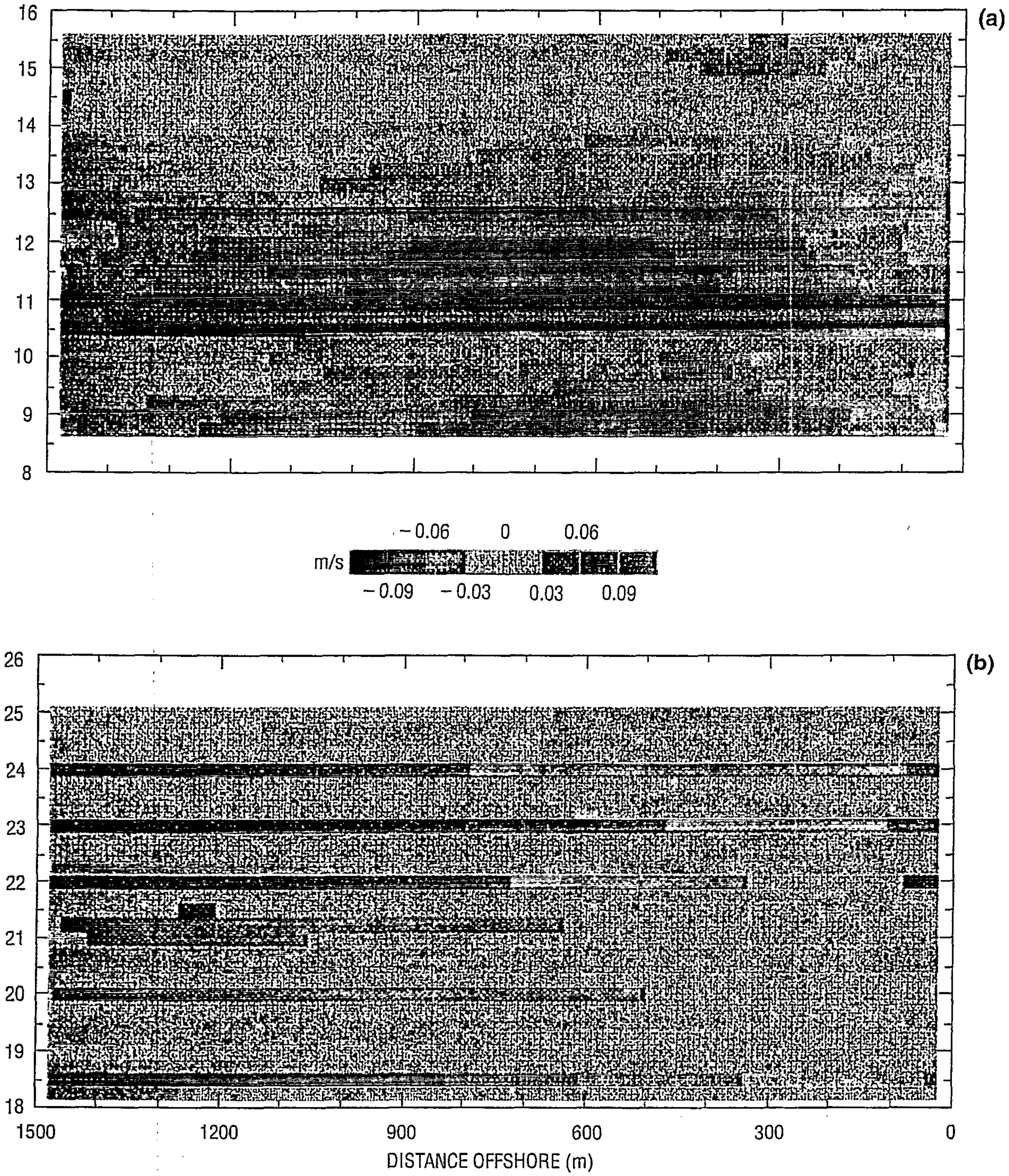

Fig. 23 — NSSM longshore current for (a) January and (b) August 1995

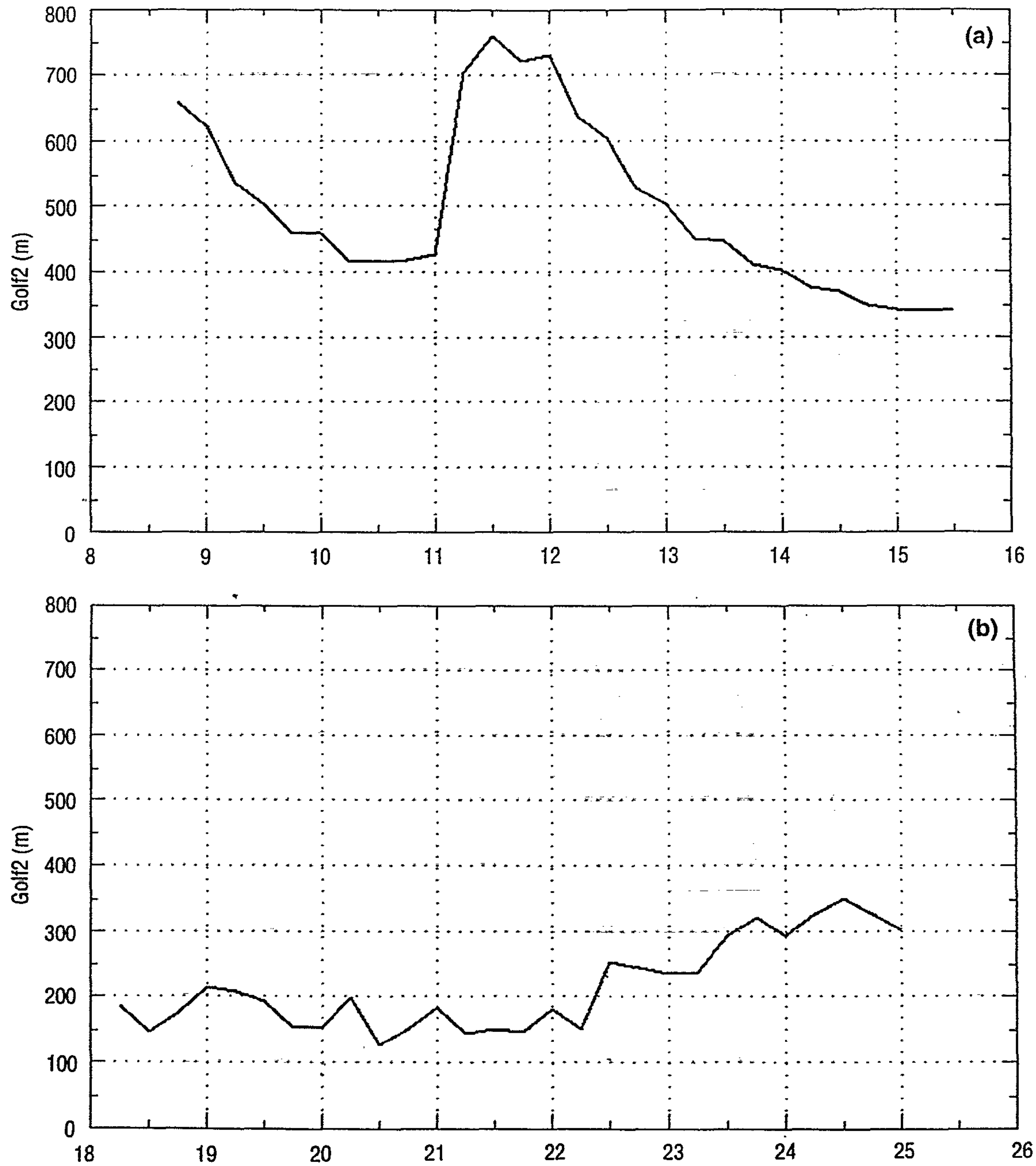

Fig. 24 — NSSM surf zone width for (a) January 1995 and (b) August 1995

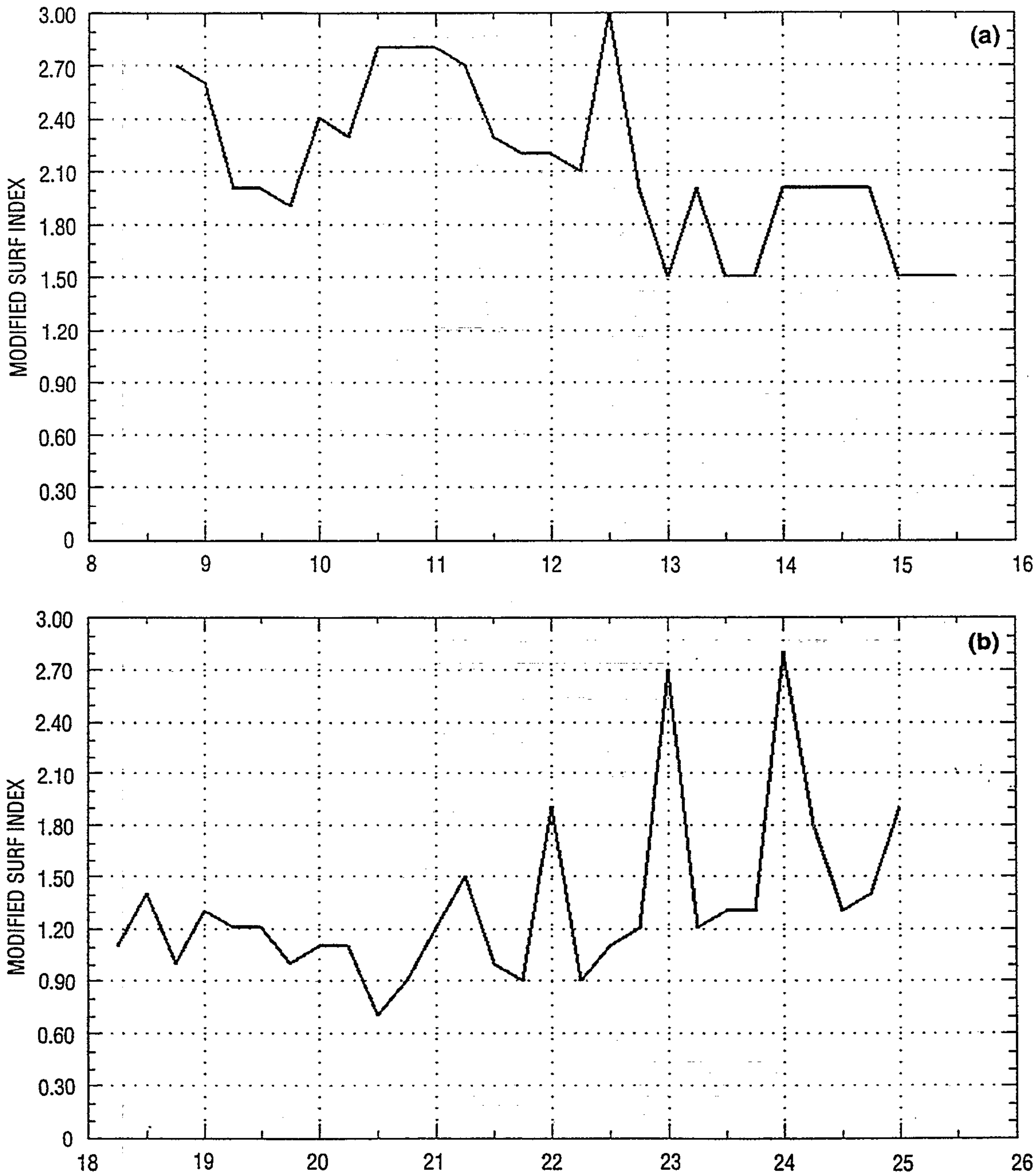

Fig. 25 — NSSM Modified Surf Index for (a) January and (b) August 1995

The modified surf index shown in Fig. 25 is an objectively determined number computed from the surf forecast and based on the *Joint Surf Manual*. It is used to determine if a safe landing by a landing craft or amphibious vehicle is possible. For example, if a landing craft or amphibious vehicle required a modified surf index less than 2.0 to make a safe landing, landing would have been risky for a majority of the time periods in January, while August would have been fine.

Figure 26 illustrates the importance of using a nearshore beach profile for NSSM modeling. Three different beaches from Camp Pendleton are plotted: the minimum slope linear beach, the maximum slope linear beach, and a representative nearshore beach extracted from the bathymetry. Three NSSM outputs—significant breaker height, dominant breaker period, and surf zone width—are listed for each beach. The dominant breaker periods are the same for each beach, but the significant breaker heights and surf zone widths differ. It is obvious that an actual nearshore beach profile will provide more realistic modeling results than a simple linear slope beach profile. In addition, the higher the resolution of the nearshore beach profile, the more realistic the NSSM results will be.

4.0 ISSUES

The basic NSSM modeling flow used for SE4 is illustrated in Fig. 27. COAMPS winds, WAM wave spectra, and hypsography were not retrieved from MEL. When modeling began, the COAMPS data had been ingested into MEL, but the WAM spectra and bathymetry had not. Software was written and run to compute wind speeds and directions from the COAMPS data at 6-h increments during the January and August 1995 time periods. The hypsography was plotted and from that plot a water depth grid for refraction was built by determining distance offshore versus water depth. In addition, a representative linear beach slope was selected after analysis of the hypsography. Lastly, tide levels were obtained from tide tables (NOAA 1995). The computed COAMPS wind speeds and

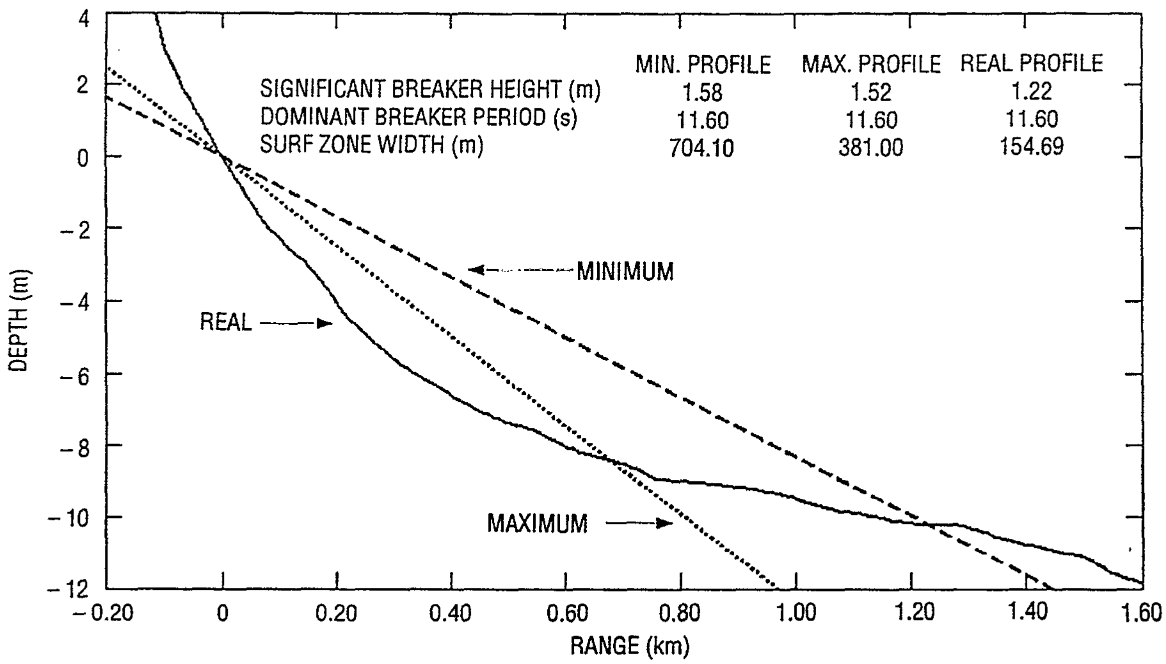

Fig. 26 — Effect of nearshore beach profile versus depth on NSSM forecast output

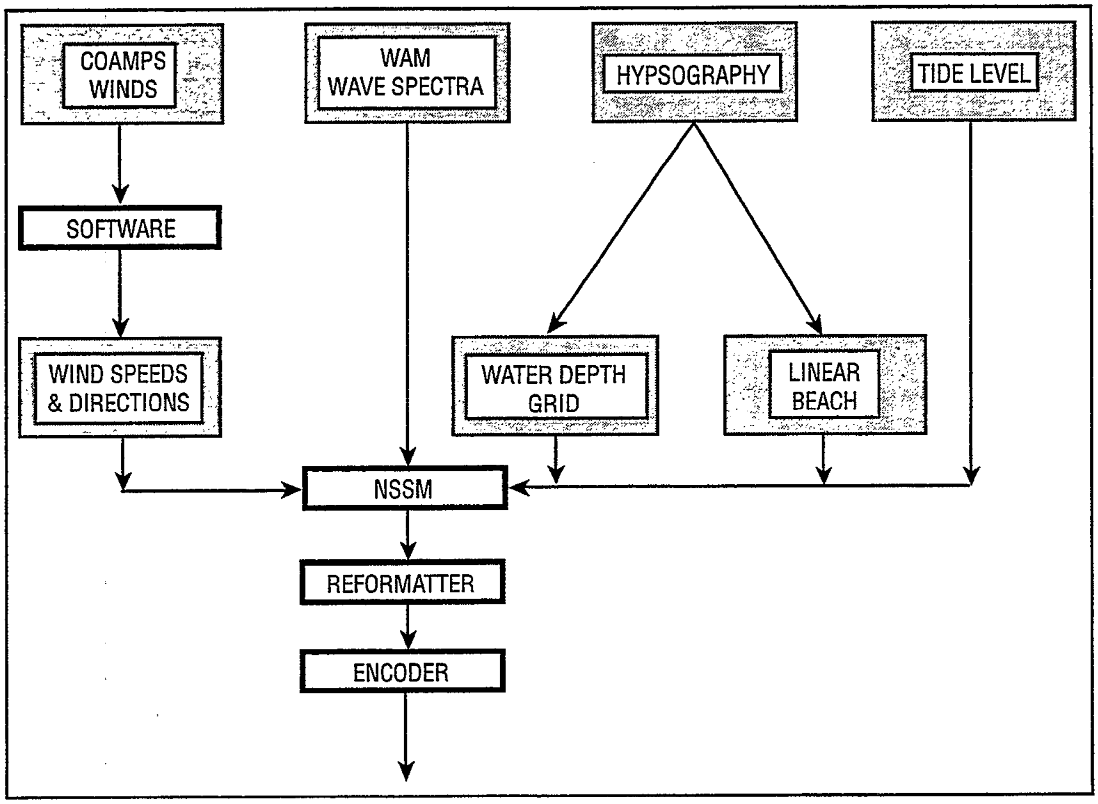

Fig. 27 — Basic NSSM modeling flow adopted for SE4

directions, WAM wave spectra, water depth grid and linear beach profile derived from the hypsography, and tide levels were fed into NSSM. NSSM was run at forecast dates/times corresponding to that of WAM. Appendix C shows a sample NSSM ASCII output for 12 Jan 1995 12Z. The detailed surf output begins at a distance of 4850 ft offshore from the Camp Pendleton beach location and increments in toward the beach at 10 ft intervals.

A reformatter code was written to take raw NSSM output (as shown in App. C), strip out the ASCII text, and write out the relevant NSSM numerical values to an ASCII file. NSSM output was provided to the Mississippi State University Center for Air-Sea Technology (MSU-CAST), which encoded the stripped ASCII NSSM output into the MEL standard BUFR (Binary Universal Format for the Representation of meteorological data) format. NSSM output subsequently obtained from MEL in BUFR format was decoded and compared with the original NSSM output. No difference was found between the two outputs.

Another issue in this modeling procedure was demonstrated by the omission of using the STWAVE spectra output as input into the NSSM runs. The FY96 effort used the deep-water WAM spectra as input into NSSM. FY97 plans call for the use of a telescoping procedure to be adopted in which the output from a regional WAM model can be fed into a shallow-water wave model (such as STWAVE); the shallow-water wave model directional spectra are then fed to the NSSM. The NSSM output is then encoded into the appropriate MEL format and made available to the modeling and simulation community. This modular approach is shown in Fig. 28.

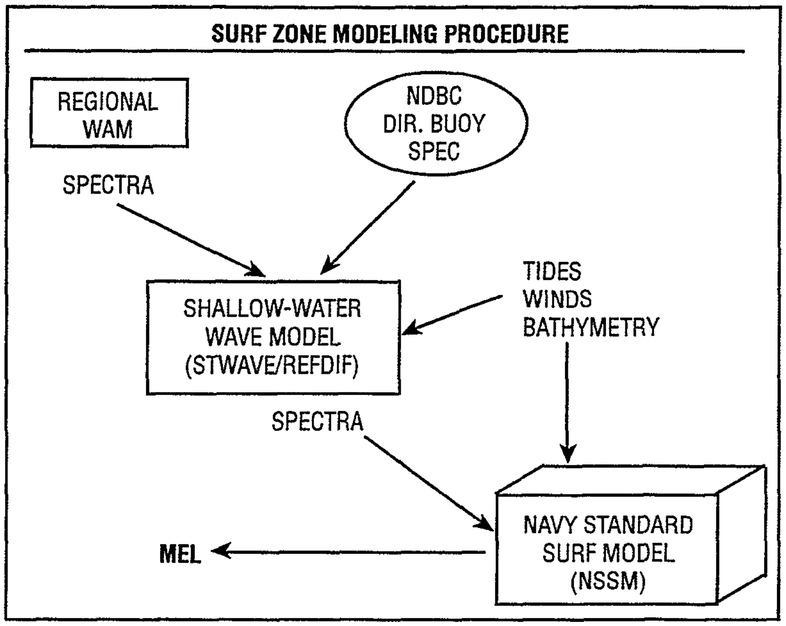

Fig. 28 — Proposed JDSZEM modeling flow for FY97 effort

5.0 SUMMARY AND RECOMMENDATIONS

This report documents the modeling procedure used during the FY96 JDSZEM Program. The approach of this program is to develop techniques that incorporate current state-of-art physics-based numerical models to determine surf zone characteristics that are important to the modeling and simulation community. To test this proof of concept, a suite of models were identified and tested at Camp Pendleton, CA, during two 7-day periods in January and August 1995. This period was chosen to coincide with the MEL's Integrated Synthetic Scenario time frame during which data from a very high-resolution atmospheric model (COAMPS) and a deep-water wave model (WAM) were already available for the Camp Pendleton, CA, area.

Spectra describing the wave energy distribution in both frequency and direction were obtained from the Southern California Regional WAM model and specified on the offshore boundary of the STWAVE shallow-water wave model. While the procedure for setting up STWAVE is straightforward, engineering judgment is required. Wave heights should be reasonable for the local depth and periods and directions should be reasonable for the possible fetches. STWAVE assumes a mild slope, so bathymetry may have to be smoothed if it is extremely steep or rugged. The STWAVE grid should be aligned as closely as possible to the bathymetric contours; nonalignment will lead to waves traveling offshore (relative to the grid) and errors in the model. STWAVE is a time-independent model. For wave simulations where the wave field changes rapidly, a time-dependent model should be considered.

STWAVE was run to coincide with the time period of available WAM and COAMPS data. To limit the scope of the modeling effort, the last 7 days during which WAM and COAMPS data were available were utilized. The STWAVE results were provided for MEL encoding.

The NSSM was run for the Camp Pendleton area for the same periods WAM and STWAVE were run; 8–14 Jan and 18–24 Aug 1995. A refraction zone depth grid was built from a 100-m resolution bathymetric data base. Inputs included COAMPS wind speed and direction, tide levels from tide tables, WAM spectra, and a landing zone based on a linear beach slope of 0.007. NSSM output was encoded into the MEL standard BUFR format and made available to the modeling and simulation community.

While the NSSM results for this exercise appear reasonable, future efforts should include coupling the STWAVE spectra directly to NSSM. The WAM model is essentially a deep-water wave model; STWAVE is designed for shallow-water applications and captures the complex refraction patterns in regions of complex bathymetry. STWAVE output can be used to construct realistic water surfaces for environmental simulations.

6.0 ACKNOWLEDGMENTS

This work was conducted under the sponsorship of the OEA and DMSO in coordination with supporting efforts at the NSWC, Panama City, FL, by Roger Leete, Robert Croft, Robert Biano, and William Littlejohn. The authors wish to thank Steve Lowe (SAIC, Monterey, CA) for providing the COAMPS dataset, Paul Farrar of NAVOCEANO for providing the WAM data, John Breckenridge of NRL for providing the bathymetry, Eileen Kennelly and Julian Richard of Neptune Sciences Inc. for providing the NSSM data, Kelley Miles of Sverdrup Technology, Inc. for providing MEL datasets, Ed Clark of MSU-CAST for MEL ingestion of the modeled data, and David Whitney (TASC, Reading, MA) for providing technical guidance associated with TAOS and the SE4 effort.

7.0 REFERENCES

Allard, R. A., P. Farrar, D. Mark, J. Martin, B. Shapiro, S. Lowe, and D. S. Ko, "Creating a 4-D Integrated Scenario Near Camp Pendleton, CA," preprints, AMS Conference on Coastal Oceanic and Atmospheric Prediction, Atlanta, GA, pp. 15–21, 1996.

Joint Surf Manual, COMNAVSURFPAC/COMNAVSURFLANT, updated 2 Jan 1987, Instruction 3840, 1B.

Davis, J. E., "STWAVE Theory and Program Documentation," Chapter 8 in Coastal Modeling System User's Manual, Instructional Report CERC-91-1, Supplement 1, M. A. Cialone (ed.), U.S. Army Corps of Engineers Waterways Experiment Station, Vicksburg, MS, 1992.

Earle, M. D., "Surf Forecasting Software Scientific Reference Manual," NORDA Technical Note 351, Naval Research Laboratory, Stennis Space Center, MS, 1989, 261 pp.

Earle, M. D., "Surf Forecasting Software User's Manual," NORDA Technical Note 352, Naval Research Laboratory, Stennis Space Center, MS, 1988, 194 pp.

Earle, M. D., "Surf Forecasting Software Improvements," MEC Systems Corp. Report, Manassas, VA, 1991.

Hodur, R. M., "Development and Testing of the Coupled Ocean/Atmosphere Mesoscale Prediction System (COAMPS)," NRL/MR/7533--93-7213, Naval Research Laboratory, Monterey, CA, 1993, 81 pp.

Komen, G. J., L. Cavaleri, M. Donelan, K. Hasselmann, S. Hasselmann, and P. A. E. M. Janssen, "Dynamics and Modelling of Ocean Waves," Cambridge University Press, Cambridge, U.K. and New York, NY, 1994, 532 pp.

Leenknecht, D. A. and W. W. Tanner, "Grid Generation and Data Analysis for Wave Transformation Models," Proceedings of the 4th Congress on Computing in Civil Engineering, Philadelphia, PA, 1997 (in press).

Mettlach, T., E. P. Kennedy, and D. May, "Surf Forecasting Using Directional Wave Spectra with the Navy Standard Surf Model," NRL/MR/7240--96-8019, Naval Research Laboratory, Stennis Space Center, MS, 1996.

Resio, D. T., "Shallow-Water Waves I: Theory," *Journal of Waterways, Ports, Coastal, and Ocean Engineering* **113**(3), 264–281 (1987).

Resio, D. T., "Shallow-Water Waves II: Data Comparisons," *Journal of Waterways, Ports, Coastal, and Ocean Engineering* **114**(1), 50–65 (1988a).

Resio, D. T., "A Steady-State Wave Model for Coastal Applications," Proceedings of the 21st Coastal Engineering Conference, ASCE, 929–940 (1988b).

Tide Tables 1995: High and Low Water Predictions, West Coast of North and South America Including the Hawaiian Islands, U.S. Department of Commerce, National Oceanic and Atmospheric Administration, National Ocean Service, 1995.

WAMDI Group, "The WAM Model—A Third-Generation Ocean Wave Prediction Model," *J. Phys. Ocean.* **18**, 1775–1810 (1988).

Appendix A

SAMPLE WAM SPECTRA

1 **0.033333**			
0.5616873E-08	0.2462234E-08	0.7670370E-09	0.2945516E-09
0.3923139E-08	0.2473300E-05	0.4119543E-07	0.2178458E-03
0.9676244E-04	0.1393732E-05	0.5840227E-08	0.8182476E-11
0.2287537E-14	0.6707154E-26	0.7365210E-33	0.4284573E-30
0.3838083E-27	0.2920183E-24	0.1905650E-21	0.1050762E-18
0.4117434E-16	0.1207638E-13	0.2473201E-11	0.2781511E-09
2 **0.036667**			
0.4310998E-06	0.2057617E-06	0.8421995E-07	0.3659017E-07
0.1132994E-06	0.2433702E-04	0.3930591E-06	0.9482045E-02
0.1082495E-02	0.1419655E-04	0.5800474E-07	0.8088462E-10
0.2265497E-13	0.8598563E-24	0.5693797E-31	0.2774535E-28
0.2501745E-25	0.1915897E-22	0.1259024E-19	0.6998700E-17
0.2751603E-14	0.8042726E-12	0.1597455E-09	0.1675065E-07
3 **0.040333**			
0.1733637E-04	0.1120020E-04	0.7274542E-05	0.2925711E-05
0.4344446E-05	0.1513987E-03	0.2558133E-05	0.2931828E-01
0.3108830E-02	0.4019208E-04	0.1635146E-06	0.2347177E-09
0.6538331E-13	0.3559924E-22	0.1360486E-29	0.6375280E-27
0.5759755E-24	0.4418972E-21	0.2908843E-18	0.1619505E-15
0.6400817E-13	0.1898046E-10	0.3845254E-08	0.4573324E-06

•
•
•

23 **0.271343**			
0.1715346E+00	0.1199340E+00	0.8180059E-01	0.5647603E-01
0.4125012E-01	0.1960179E-01	0.5880949E-02	0.1836945E-02
0.2085777E-03	0.2093702E-05	0.8811795E-08	0.1663658E-10
0.5823969E-14	0.9190807E-15	0.1227561E-11	0.1000435E-08
0.4461096E-06	0.1785736E-04	0.2880798E-03	0.4838678E-02
0.2662352E-01	0.7806841E-01	0.1393448E+00	0.1873751E+00
24 **0.298477**			
0.1098788E+00	0.8918653E-01	0.6823354E-01	0.4561832E-01
0.3112438E-01	0.1773810E-01	0.5545077E-02	0.8520262E-03
0.1199325E-03	0.1245529E-05	0.5373998E-08	0.1073234E-10
0.3826144E-14	0.6195230E-15	0.8841187E-12	0.7492055E-09
0.3382069E-06	0.1404922E-04	0.2861711E-03	0.5081573E-02
0.2706281E-01	0.7168264E-01	0.1062097E+00	0.1204870E+00

25 **0.328325**

0.7778282E-01	0.6453511E-01	0.4950420E-01	0.3332744E-01
0.2371782E-01	0.1506255E-01	0.4153857E-02	0.3709494E-03
0.5095717E-04	0.5869923E-06	0.2642540E-08	0.5803019E-11
0.2115476E-14	0.3921677E-15	0.6061717E-12	0.5434094E-09
0.2525598E-06	0.1182036E-04	0.3487615E-03	0.6149069E-02
0.2700221E-01	0.5207186E-01	0.7025708E-01	0.8295534E-01

APPENDIX B

SAMPLE STWAVE OPTIONS FILE

```
  121     191     25     35    100.000    0      0    1856
0.0333  0.0367  0.0403  0.0444  0.0488  0.0537  0.0591  0.0650  0.0715  0.0786
0.0865  0.0951  0.1046  0.1151  0.1266  0.1392  0.1532  0.1685  0.1853  0.2039
0.2243  0.2467  0.2713  0.2985  0.3283
 100,  1,  9.600889999999993
 101,  1,  8.291029999999978
 102,  1,  6.864949999999993
 103,  1,  5.770280000000014
 104,  1,  4.960219999999993
 105,  1,  4.455990000000014
 106,  1,  2.568399999999997
 107,  1,  0.914199
 108,  1,  0.1364879999999999
 109,  1,  0.6447140000000005
 100,  2,  9.565719999999999
 101,  2,  8.572499999999991
 102,  2,  7.972829999999988
 103,  2,  6.48442
 104,  2,  4.725799999999992
 105,  2,  3.59545
 106,  2,  2.700069999999997
 107,  2,  1.24718
 108,  2,  0.3527970000000007
 109,  2,  0.2164520000000003
 110,  2,  0.6130780000000016
 100,  3,  9.746359999999981
 101,  3,  8.945460000000026
 102,  3,  8.177329999999984
 103,  3,  7.356519999999989
 104,  3,  5.933909999999997
 105,  3,  4.387290000000007
 106,  3,  2.771709999999999
 107,  3,  0.9743180000000002
 110,  3,  0.2910850000000007
 100,  4,  9.874810000000025
 101,  4,  9.043810000000008
```

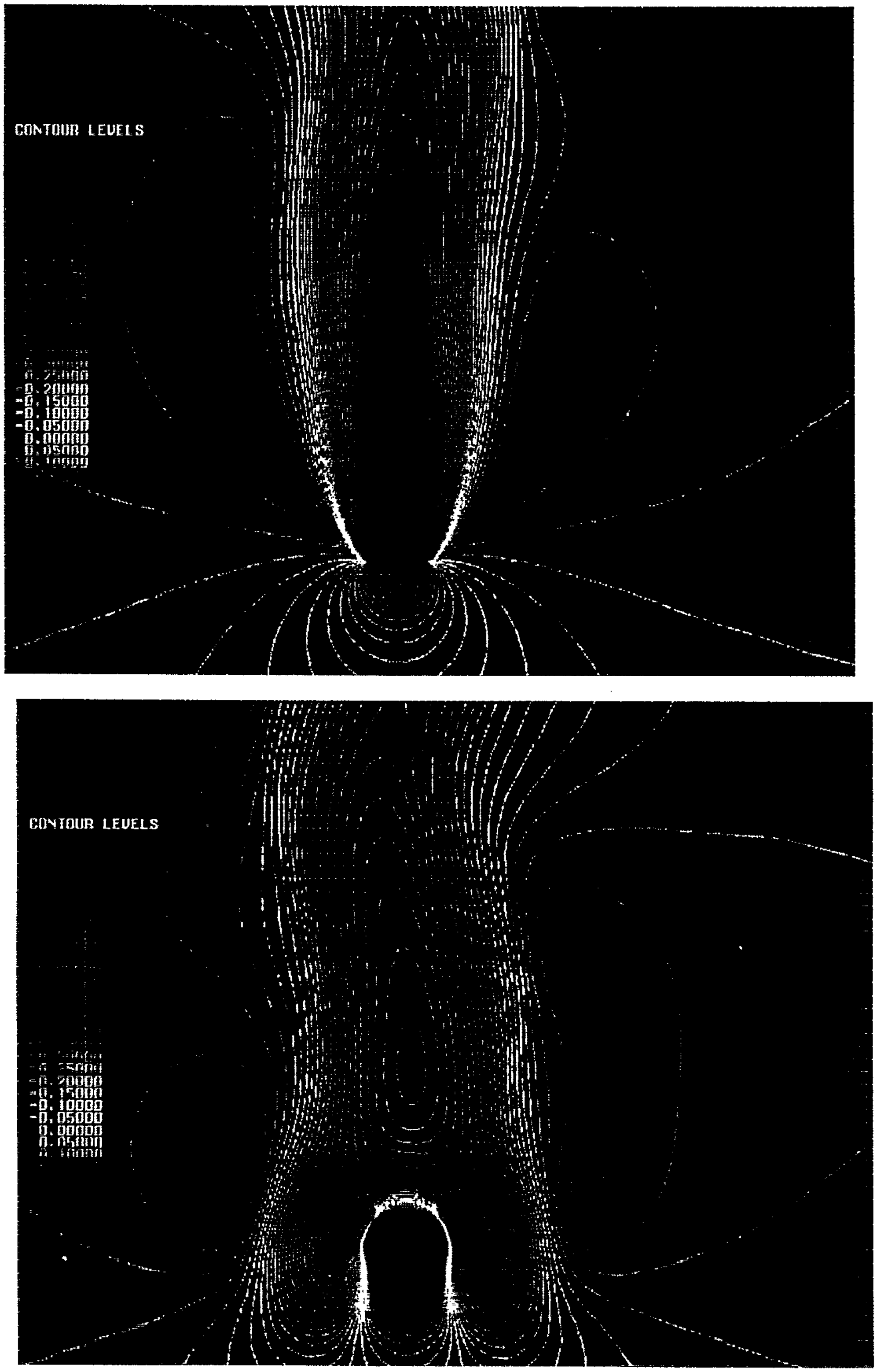

Fig. 18 — Contours of vertical velocity for initial certification studies (see text for explanation)